bioRχiv

Nutritional state-dependent modulation of Insulin-Producing Cells in *Drosophila*

Rituja S. Bisen[1], Fathima Mukthar Iqbal[1], Federico Cascino-Milani[1], Till Bockemühl[2], and Jan M. Ache[1, *, ‡]
[1]Neurobiology and Genetics, Theodor-Boveri-Institute, Biocenter, Julius-Maximilians-University of Würzburg, Würzburg, 97074, Germany
[2]Institute of Zoology, Department of Biology, University of Cologne, 50674 Cologne, Germany
*Address for correspondence: jan.ache@uni-wuerzburg.de
‡Lead Contact

Insulin plays a key role in regulating metabolic homeostasis across vertebrate and invertebrate species. *Drosophila* Insulin-Producing Cells (IPCs) are functional analogues to mammalian pancreatic beta cells and release insulin directly into circulation. IPC activity is modulated by nutrient availability, circadian time, and the behavioral state of animals. To investigate the *in vivo* dynamics of IPC activity in the context of metabolic homeostasis, we quantified effects of nutritional and internal state changes on IPCs using electrophysiological recordings. We found that the nutritional state strongly modulates IPC activity. IPCs were less active in starved flies than in fed flies. Refeeding starved flies with glucose significantly increased IPC activity, suggesting that IPCs are regulated by hemolymph sugar levels. In contrast to glucose feeding, glucose perfusion had no effect on IPC activity. This was reminiscent of the mammalian incretin effect, in which ingestion of glucose drives higher insulin release than intravenous glucose application. Contrary to IPCs, Diuretic hormone 44-expressing neurons in the pars intercerebralis (DH44^{PI}Ns), which are anatomically similar to IPCs, significantly increased their activity during glucose perfusion. Functional connectivity experiments based on optogenetic activation demonstrated that glucose-sensing DH44^{PI}Ns do not affect IPC activity, while other DH44Ns inhibit IPCs. This suggests that populations of autonomously and systemically glucose-sensing neurons are working in parallel to maintain metabolic homeostasis. Ultimately, metabolic state changes affect animal behavior. For example, hungry flies increase their locomotor activity in search of food to maintain metabolic homeostasis. In support of this idea, activating IPCs had a small, satiety-like effect in starved flies, resulting in reduced walking activity, whereas activating DH44Ns strongly increased walking activity. Taken together, we show that IPCs and DH44Ns are an integral part of a sophisticated modulatory network that orchestrates glucose homeostasis and adaptive behavior in response to shifts in the metabolic state.

Introduction

Insulin is a key neuropeptide that controls metabolic homeostasis across the animal kingdom[1–4]. Beyond metabolic homeostasis, insulin signaling is implicated in physiological processes underlying reproduction, aging, and stress resistance[5–7]. When nutrients are abundant, insulin promotes the uptake and storage of energy. Conversely, during periods of starvation, insulin release is downregulated[8,9], which promotes the conservation of energy resources and enables energy mobilization via counter-regulatory pathways[10–12]. Maintaining this energy balance is vital for survival. Accordingly, dysregulation of this finely tuned system is a hallmark of metabolic disorders such as type 2 diabetes[13–15].

Drosophila melanogaster has emerged as a model system to study insulin signaling because of the availability of a powerful genetic toolkit[16–21]. In *Drosophila*, Insulin-Producing Cells (IPCs), which are analogous to human pancreatic beta cells, reside in the pars intercerebralis (PI) of the brain[22]. These IPCs secrete *Drosophila* insulin-like peptides (DILPs) and are sensitive to changes in the metabolic state[23–26], the behavioral state[27,28], the circadian time[25,29], aminergic and peptidergic inputs[30], and other peripheral signals[31]. Consequently, they play a key role in orchestrating the metabolic demands of behaving animals. For instance, insulin acts as a global cue for modulating odor-driven food-search in accordance with a fly's nutritional state[32]. Unlike pancreatic beta cells, IPCs are localized in the brain and engage in direct synaptic signalling[33] in addition to endocrine signalling. Thus, IPCs are part of a complex system that integrates both neuronal and peripheral signals. As a key hub integrating metabolic state information, IPCs are thought to be part of the neuronal circuitry that regulates food intake[32,34–39], in part by regulating foraging behavior. Previous studies found that octopamine, the insect analogue to norepinephrine, mediates starvation-induced hyperactivity in flies[38]. A subset of octopaminergic neurons expressing *Drosophila* insulin receptor (dInR) are necessary to regulate starvation-induced hyperactivity[38,40] implicating that IPCs play a role in modulating foraging behavior.

While much is known about carbohydrate metabolism and insulin signaling in *Drosophila*[5,28,41,42], the *in vivo* dynamics of IPCs remain largely elusive. *Ex vivo* studies indicate that IPCs themselves are sensitive to glucose, as evidenced by increased firing rates upon glucose application[23,43]. However, the influence of feeding and nutritional states on IPC activity *in vivo*, as well as the nutritional state-dependent response of IPCs to glucose, remain unclear, underscoring the importance of *in*

vivo studies where all nutrient-sensing and sensorimotor circuits are intact. For instance, how does IPC activity differ when glucose is ingested as part of a meal, compared to when glucose is administered directly to the brain or into circulation? In mammalian systems, insulin release is significantly amplified upon glucose ingestion vs. intravenous administration[44,45], a phenomenon known as the 'incretin effect' [46,47]. This underlines the complexities of insulin regulation, emphasizing that insulin secretion is not solely dictated by sugar levels but influenced by multiple factors. Here, we investigated the nutritional state-dependent modulation of IPCs in *Drosophila* using an *in vivo* electrophysiological approach.

We recently demonstrated that IPC activity is strongly modulated by locomotion on fast timescales[27]. Whether the converse is true, and IPC activity can directly affect behavior on short timescales, is not clear. To address this, we optogenetically manipulated IPCs and other modulatory neurons while recording the locomotor activity of freely walking flies.

Overall, we demonstrate that IPC activity is not just nutritional state-dependent, but that IPCs also exhibit an incretin-like effect. We further establish that the nutritional state strongly modulates locomotor activity, and that IPCs play a small but significant role in this. In addition, we confirm that another set of modulatory neurons adjacent to the IPCs, DH44^{PI}Ns, are sensitive to glucose perfusion. While DH44^{PI}Ns do not affect IPC activity on short-timescales, DH44 neurons outside the PI (DH44Ns) form strong inhibitory connections to IPCs. These DH44Ns also have strong effects on locomotor activity, which are antagonistic to those of IPCs. Our findings imply distinct mechanisms by which IPCs and DH44^{PI}Ns sense changes in nutritional state, underlining the significance of multiple pathways in orchestrating *Drosophila's* response to nutritional state changes and ensuring metabolic homeostasis.

Results

IPC activity is modulated by the nutritional state

To characterize the electrophysiological activity of IPCs in different nutritional states, we performed *in vivo* patch-clamp recordings from IPCs in fed and starved *Drosophila* (Figure 1A-C). First, flies were fed *ad libitum*, and the IPC baseline activity was determined by recording their spontaneous activity in glucose-free extracellular saline over 10 minutes. The baseline firing rate varied between individual IPCs and ranged from 0 to 1.4 Hz (Figure 1D). To assess the effect of starvation on IPC activity, we wet-starved flies for 24 hours. IPCs in starved flies were significantly less active, and basically remained quiescent with 14 out of 16 IPCs recorded (88%) exhibiting a firing rate of 0 Hz (Figure 1D). We also analyzed the resting membrane potential (V_m) of IPCs in fed and starved flies. On average, the V_m of IPCs was 9 mV more depolarized (median: -50 mV) in fed flies compared to starved flies (median: -59 mV, Figure 1E). This indicates a higher excitability of IPCs after feeding, which likely explains their higher firing rates. These results demonstrate that IPC activity and hence insulin release are strongly modulated by the nutritional state.

Since IPCs are central to metabolic regulation and development, factors other than the nutritional state may impact their activity. To address two of the key factors, we analyzed whether IPC activity was affected by the mating state or the age of the fly. The IPC activity in virgin flies was slightly lower than that of mated females, but this difference was not significant (Supplementary Figure S1A). Although IPC activity was highest in males, there were no significant differences between the three groups (Supplementary Figure S1A). Hence, IPC activity is not significantly affected by sex or female mating state. However, when recording the IPC activity in females of different age groups, we observed that IPCs remained almost quiescent in fully fed females older than ten days. Here, baseline spike rates ranged from 0 – 0.2 Hz and were significantly lower than in younger females (Supplementary Figure S1B). This indicates that IPC activity is suppressed in older flies. Therefore, aging significantly reduces IPC activity.

IPCs are sensitive to glucose ingestion

To investigate whether and how IPC activity is modulated by nutrient uptake *in vivo*, we starved flies for 24 h and then refed them with a high glucose (HG) diet (400 mM glucose in 2% agar) for durations between 3 to 24 h (Figure 1F). IPC activity in flies that were refed for 3-5 h resembled that of starved flies and remained around 0 Hz (Figure 1G). Six hours after the start of refeeding, IPC activity started to increase, and was indistinguishable from that of fed flies (Figure 1G, $p = 0.68$), indicating that this duration was sufficient to allow IPC activity to fully recover from starvation. Interestingly, IPC activity kept increasing for longer glucose feeding durations, and was significantly increased in flies that were refed with glucose for 18-24 h compared to flies kept on a full diet and fed *ad libitum* (Figure 1G, $p = 0.02$). This indicates that the release of insulin from IPCs increased when flies were exclusively feeding on glucose. We conclude that IPC activity was increased in flies feeding on a pure sugar diet, and that the temporal dynamics of this effect were relatively slow.

Next, we asked whether the increased IPC activity after refeeding was glucose-specific or a general response to food intake. To test this, we kept 24 h starved flies on either a standard (SD) or high protein diet (HP) and compared the IPC activity after refeeding for 18-24 h. In contrast to refeeding flies with HG diets, refeeding them with either HP or SD diets caused no significant increase in the spike rate of IPCs compared to starved flies ($p = 0.43$ and 0.77, respectively, Figure 1H). This was intriguing, because both protein-rich diets and full diets have been shown to induce insulin secretion under fed conditions[26,48,49]. To ensure that these results were not due to a lasting interference with the fly's metabolic system caused by keeping the flies on an extreme diet, we conducted a survival assay. Analogous to our electrophysiology experiments, we starved the flies for 24 h and then refed them on HG, SP, or SD. Subsequently, we monitored the number of survivors every day while flipping flies onto fresh food every second day. As expected, flies fed with SD survived the longest (100 % survival until day 43, Supplementary Figure S1C). 100 % survival was observed for flies fed with HG until Day 12 and at least half of the flies survived until day 16 (Supplementary Figure S1C). In comparison, flies survived poorly on HP diet: 100 % survival was observed only up to day 1 and more than half of the flies were dead by day 12 (42.5 % survival, Supplementary Figure S1C). Since our IPC recordings were acquired in flies refed on HP or HG for a maximum of 24 hours, the effects we observed on IPC activity were not due to lethality in flies but rather due to differences in nutrient availability. Hence, we conclude that the increase in IPC activity after refeeding was indeed glucose specific.

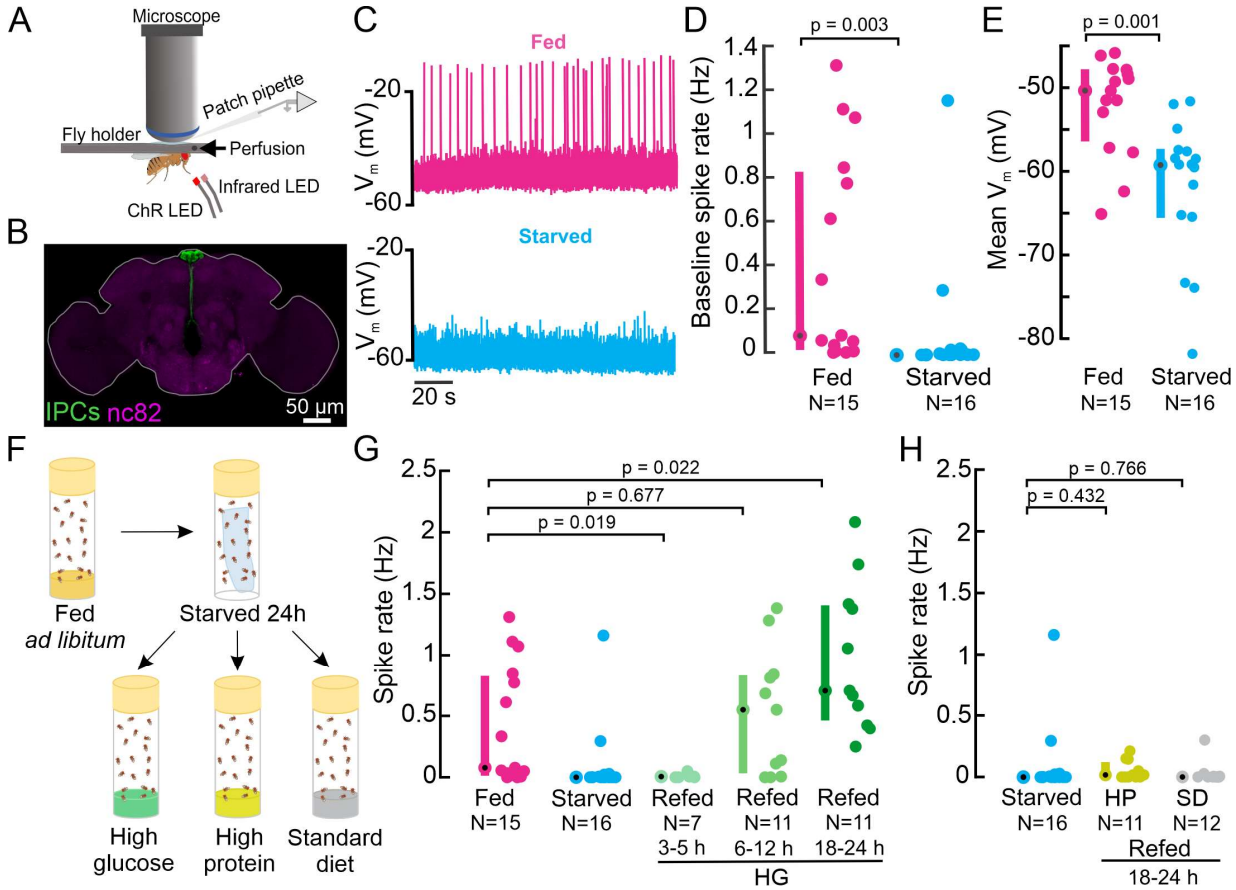

Figure 1: IPC activity depends on the nutritional state and increases after glucose ingestion.
A) Schematic of the setup for *in vivo* IPC whole cell patch-clamp recordings. **B)** IPCs in the *Drosophila* brain. *UAS-myr-GFP* was expressed under a *Dilp2-GAL4* driver to label IPCs. The GFP signal was enhanced with anti-GFP (green), brain neuropils were stained with anti-nc82 (magenta). **C)** Representative examples of the membrane potential of two IPCs recorded in fed (magenta) and starved (cyan) flies. **D)** Average baseline spike rate and **E)** membrane potential of IPCs in fed (magenta) and starved (cyan) flies. Each dot represents an individual IPC, error bars indicate median (circle) and inter-quartile range (IQR, bars). P-values from Wilcoxon rank-sum test. **F)** Schematic of the experimental starvation and refeeding protocol. HG: High glucose, HP: High protein, SD: Standard diet. **G)** Comparison of IPC spike rates in fed flies (magenta), 24 h starved flies (cyan), and flies refed on HG for different durations (green). **H)** Comparison of IPC spike rate in 24 h starved flies (cyan), HP (yellow) and SD (grey). Each circle represents an individual IPC, N = number of IPCs (at least 7 flies were used for each condition).

The nutritional state affects locomotor activity

Starvation increases baseline locomotor activity in flies and other animals. This 'starvation-induced hyperactivity' is a hallmark of foraging behavior[32,38,40,50–53] as it enables animals to explore their environment and locate food sources. As major integrators of metabolic state information, IPCs are thought to be part of the neuronal circuitry that modulates foraging[40]. For example, insulin inhibits a subset of olfactory sensory neurons, such that decreased insulin release leads to an increase in sensitivity to food odors[54]. Our findings that IPC activity is directly modulated by starvation and feeding support the hypothesis that they are part of the neuronal networks modulating foraging. To further investigate the relationship between nutritional states, IPC activity, and foraging behavior, we used our 'Universal Fly Observatory' (UFO) setup to quantify locomotor activity[55], in in particular starvation-induced hyperactivity (Figure 2A). In the UFO, flies can walk freely in a circular arena illuminated by infrared LEDs, and their walking activity can be quantified using semi-automated tracking software and analysis (based on the Caltech Fly Tracker[56], see Methods, Figure 2A).

To test whether IPCs play a causal role in modulating starvation-induced hyperactivity, we first quantified the effects of nutritional manipulations on walking behavior. Fully fed flies, which have elevated IPC activity, displayed a low baseline walking activity with a median FV of 0.3 mm/s (Figure 2B). 24 h starved flies, in which IPC activity was significantly reduced, were more hyperactive and displayed a significantly increased median FV of 1.9 mm/s (Figure 2B). Refeeding flies on a pure-diet for 24 h after starvation, which led to a drastic increase in-IPC activity reduced the hyperactivity by about 50% (median 0.9 mm/s) compared to starved flies (Figure 2B). Hence, the hyperactivity was significantly reduced but not abolished, despite the fact that IPC activity was maximal in these flies (Figure 1G). One interpretation of this behavior is that flies are searching for protein sources. Flies refed on a full diet (SD) were even less active than flies fed *ad libitum* before undergoing starvation, and this difference was significant (Figure 2B). These results show that the locomotor activity was affected by the same dietary manipulations that had strong effects on IPC activity. However, IPC activity changes alone cannot fully explain the modulation of starvation induced hyperactivity, since high-glucose diets which drove the highest activity in IPCs were not sufficient to reduce locomotor activity back to baseline levels. This suggests that the modulation of starvation-induced hyperactivity is achieved by multiple modulatory systems.

Next, we investigated the temporal dynamics of the modulation of locomotor activity. Since nutritional state-dependent modulation of IPC activity occurred on a relatively slow timescale over several hours to days, we tested whether starvation-induced hyperactivity was modulated on a similar

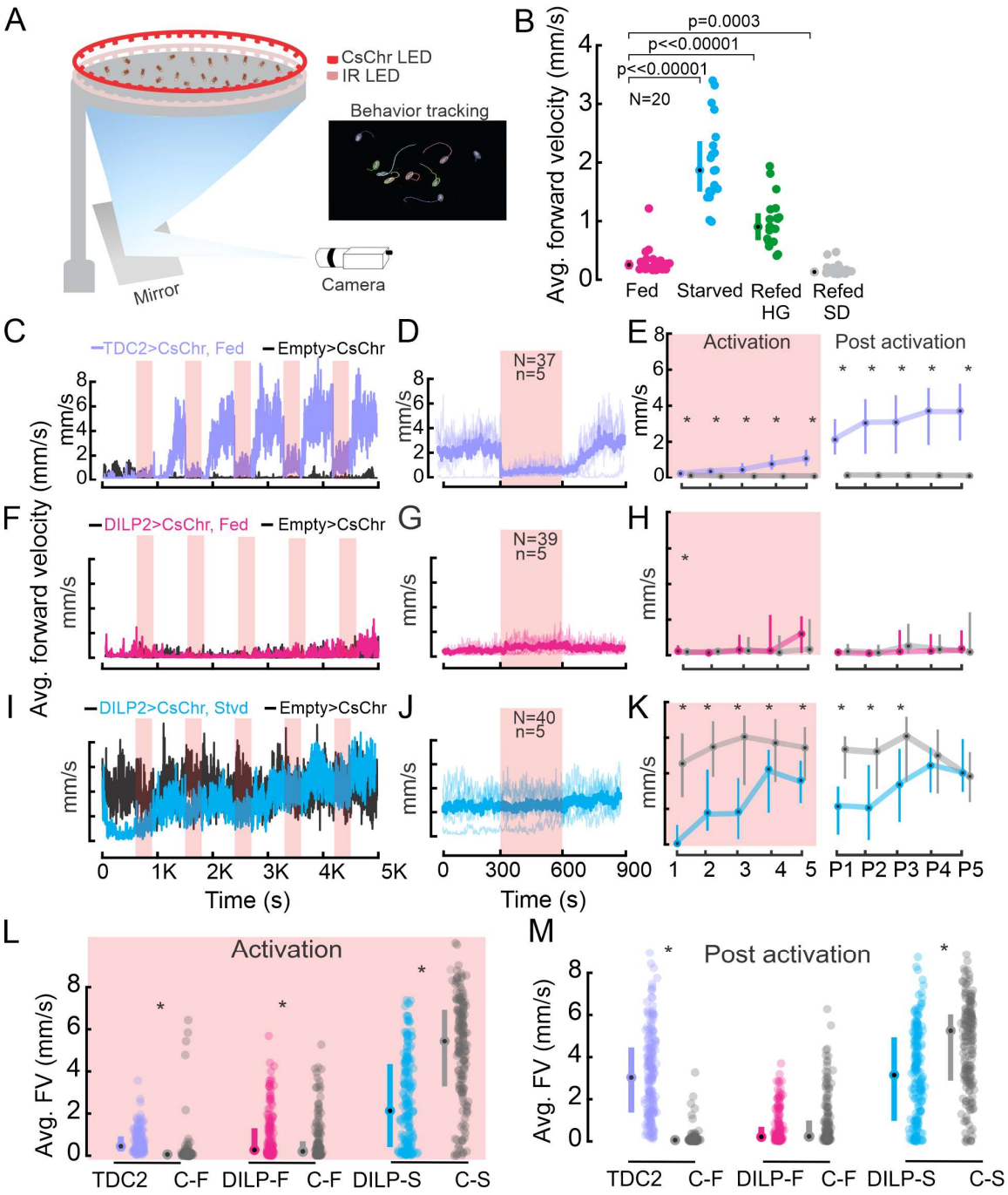

Figure 2: Walking activity is modulated by the nutritional state, OANs and IPCs.
A) Schematic showing the UFO setup. **B)** Average forward velocity (FV) of flies in different feeding states. Median and IQR are presented. p-values from Wilcoxon rank-sum test. **C)** Average FV of flies representing one replicate during optogenetic activation of OANs, in fed flies. *Empty-GAL4* was used as control for all experiments (black). Red shading, optogenetic activation (300 s each). **D)** Average FV across all trials from two replicates for OAN activation: 300s before light onset, during stimulus, and after light offset. N = number of flies, n = number of activation trials. Thin lines represent individual trials, thick lines represent median of all trials. **E)** Average FV of all flies while activating OANs. Left: each stimulus trial (1-5) and Right: 300s after light offset (P1-P5). **F)** Average FV of flies representing one replicate during optogenetic activation of IPCs in fed flies. **G)** Average FV across all trials from two replicates for IPC activation in fed flies (detailed information as in D). **H)** Average FV of all flies while activating IPCs in fed flies (detailed information as in E). **I)** Average FV of flies representing one replicate during optogenetic activation of IPCs in starved flies. **J)** Average of FV across all trials from two replicates for IPC activation in starved flies (detailed information as in D). **K)** Average FV of all flies while activating IPCs in starved flies (detailed information as in K). **L)** and **M)** Average FV pooled across all activation trials (1-5) and post activation windows (P1-P5), respectively. Median and IQR are presented. p-values from Wilcoxon rank-sum test. Where no detailed p-value is stated, asterisks represent statistical significance. See also Table S1 and S2.

timescale. To this end, we quantified the walking activity of flies that were either fed *ad libitum* or starved for increasing durations, ranging from 30 minutes to 48 hours. As established earlier, flies that were fully fed or merely starved for 30 minutes had a low FV of 0.3 mm/s (Supplementary Figure S2A). However, their walking activity increased with increasing starvation duration up to 20 hours, when it reached a maximum at an FV of 3.6 mm/s (mean, Supplementary Figure 2A). The FV of flies starved for over 20 hours decreased again, probably due to a lack of energy reserves. We observed a final peak after 36 hours of starvation (Supplementary Figure S2A), which we interpret

as a surge in starvation-induced hyperactivity before the metabolic state becomes critical. These results demonstrate that the starvation duration has a strong effect on locomotor activity, the modulation of which happens on a similar timescale as IPC modulation by changes in nutritional state.

Activation of octopaminergic neurons increases locomotor activity

Since changes in IPC activity alone were insufficient to explain starvation-induced hyperactivity, we next investigated which component of the behavioral changes were caused by IPCs and how strong their contribution was compared to other modulatory neurons. To accomplish this, we first activated octopaminergic neurons (OANs). Octopamine is the insect analogue to norepinephrine and is known to be released during flight, a metabolically demanding activity in *Drosophila*[57,58], and to induce hyperactivity in starved flies[40]. Hence, we expected OANs to drive an increase in locomotor activity, rendering them a useful reference point. We used a tyrosine decarboxylase 2 (TDC2) driver line to acutely activate OANs via the optogenetic effector CsChrimson[59] in the UFO while tracking the walking activity of flies. TDC2 is required for octopamine synthesis from tyramine[60], therefore, *TDC2-GAL4* labels all neurons producing octopamine and tyramine. In parallel, we used *empty split-GAL4*[61] flies crossed to UAS-CsChrimson as controls, which were simultaneously exposed to the same activation protocol in an adjacent UFO. This setup allowed us to account for activity changes due the red light used for optogenetic activation and other factors potentially affecting walking activity, such as small fluctuations in temperature, humidity, or differences in the circadian time. Each optogenetic activation experiment consisted of five activation cycles, in which we activated the neurons for 300 s, followed by an inter-stimulus-interval of 600 s, which we refer to as the 'post activation' window. Results reported here were analyzed by averaging two replicates per experiment.

We observed a strong, significant increase in FV from 0.23 mm/s (median) before OAN activation to 3.68 mm/s after five activation cycles, with a notable increase after each activation (Figure 2C and 2E, $p < 0.001$, see Supplementary Table S1 and S2). Notably, the final FV reached after OAN activation was comparable to that after 24 h of starvation (compare Figure 2E to starved controls in Figure 2B and I). This suggests that OAN activity can explain a large proportion of the starvation-induced hyperactivity. Interestingly, we observed a dramatic drop in FV at the onset of OAN activation (Figure 2D and 2E), during which the median FV dropped by 2 mm/s and approached 0 mm/s. This reduction in FV was due to recurring stopping behavior observed during acute OAN activation (Supplementary Figure S2B, Supplementary video S1). These behavioral effects of OAN activation have been previously described in adult flies as inhibition of food tracking via ventral unpaired median OANs and have been linked to suppression of long-distance foraging behavior[62]. Since these are not the only neurons we activate while activating tdc2 positive neurons, we speculate that the stopping phenotype could also result from concerted effects of octopamine and tyramine modulating muscle contractions, as previously described in *Drosophila* larvae[63–65], or of OANs interfering with pattern generating networks in the ventral nerve cord (VNC) during long activation[66]. Overall, long-term optogenetic activation of OANs had a strong and significant effect on walking activity and mimicked the starvation-induced hyperactivity (Figure 2I and 2K, black and gray controls).

IPC activation slightly reduces starvation-induced hyperactivity

Having confirmed a strong effect of OANs on locomotor activity and the validity of our approach, we next examined the effects of IPCs on locomotor activity in response to changes in nutritional state. To achieve this, we optogenetically activated IPCs in freely walking flies, which were either fed *ad libitum* or wet-starved for 24 h. IPC activation in fed flies had only minor effects on the FV, indicating that IPCs do not drive starvation-induced hyperactivity or other aspects of foraging behavior (Figure 2F-H). The FV of most flies remained below 2 mm/s throughout the experiment (75th percentile, Figure 2H: see 1-5 and P1-P5) and was indistinguishable from the FV of controls during all but the first activation cycle (Figure 2F and 2H: $p > 0.05$). Accordingly, their FV did not differ during most activation windows (Median (1-5) = 0 - 0.5 mm/s, Figure 2H) or post-activation windows (Median (P1-P5) = 0 - 0.1 mm/s). One exception was the first activation cycle, in which the IPC-activated flies walked slightly but significantly faster than controls (Figure 2H, 1: $p = 0.03$). When averaging the activity of all flies across all activation windows, there was a small but statistically significant difference of 0.06 mm/s (Figure 2L, $p= 0.01$). In the post-activation windows, however, the FV of IPC activated and control flies were indistinguishable (Figure 2M). Overall, IPC activation had no notable effects on locomotor activity in fully fed flies.

Next, we tested the effect of IPCs on starvation-induced hyperactivity. Given that higher IPC activity levels are associated with the fed state, we expected that activating IPCs would reduce hyperactivity in starved flies. As previously observed (Figure 1B), starved flies were generally more active than their fed counterparts and walked with a median FV ≥ 2 mm/s (Figure 2I and K). The FV of flies during IPC activation remained significantly lower than the control flies over the course of all five activation cycles (Figure 2I-K, $p < 0.05$, Supplementary Table S1). This confirmed our hypothesis that IPC activation reduces starvation-induced hyperactivity. However, two observations were counterintuitive: First, the FV of IPC activated flies and control flies converged over time, and there was no significant difference in the control and IPC-activated flies during the last two post activation windows (Figure 2I, and2K: P4, P5: $p = 0.23$ and $p = 0.45$, see also Supplementary Table S2). Hence, while activation of IPCs reduced hyperactivity, this effect did not persist after long-term activation. Second, we noted a decrease in the FV of IPC-activated starved flies even before the first optogentic stimulation (Figure 2I), possibly due to CsChrimson sensitivity to visible light. Overall, these results suggest that IPCs have a small but significant effect on behavior, in that they slightly reduced starvation-induced hyperactivity. We conclude that starvation-induced hyperactivity is affected by IPCs, but predominantly controlled by populations of modulatory neurons other than IPCs, for instance, OANs.

IPCs do not sense changes in extracellular glucose levels *in vivo*

Our experiments established that IPC activity is modulated by the nutritional state and that IPCs are sensitive to glucose ingestion, similar to pancreatic beta cells. Like beta cells, IPCs have been suggested to directly sense changes in extracellular glucose concentration in *ex vivo* studies[23,43], where IPC activity increased in response to the application of saline containing a high-glucose concentration to the nervous system. Consequently, IPCs are thought to sense extracellular glucose increases cell-autonomously. To test this hypothesis in flies with fully intact sensory and central circuits, we recorded from IPCs *in vivo*, while perfusing extracellular saline containing high concentrations of glucose over the brain. After recording the IPC baseline activity in starved flies under perfusion of glucose-free saline (Figure 3A), we perfused the brain with saline containing 40 mM glucose (Figure 3A and 3B). Similar to our previous experiments, IPC spike rates were very low with a median of 0.05 Hz after starvation. Surprisingly, perfusing high concentrations of glucose over the brain did not increase IPC activity in starved flies (Figure 3B), even after 20 minutes of perfusion. In fed flies too, glucose perfusion had no effects on the IPC activity (Supplementary Figure S3A). Towards the end of each recording session, we injected current to establish that the IPCs were still excitable.

Our findings clearly show that IPCs do not directly sense glucose in their extracellular environment *in vivo*, but rather respond to glucose ingestion during feeding (Figure 3C). Hence, IPCs require input from the gut or other sensory pathways, such as taste or mechanosensation, to release insulin in response to glucose ingestion. Taken together, the increase in IPC activity following glucose ingestion but not glucose perfusion resembles the 'incretin effect' observed in mammals, where insulin secretion is significantly higher when glucose is ingested orally compared to isoglycemic intravenous delivery

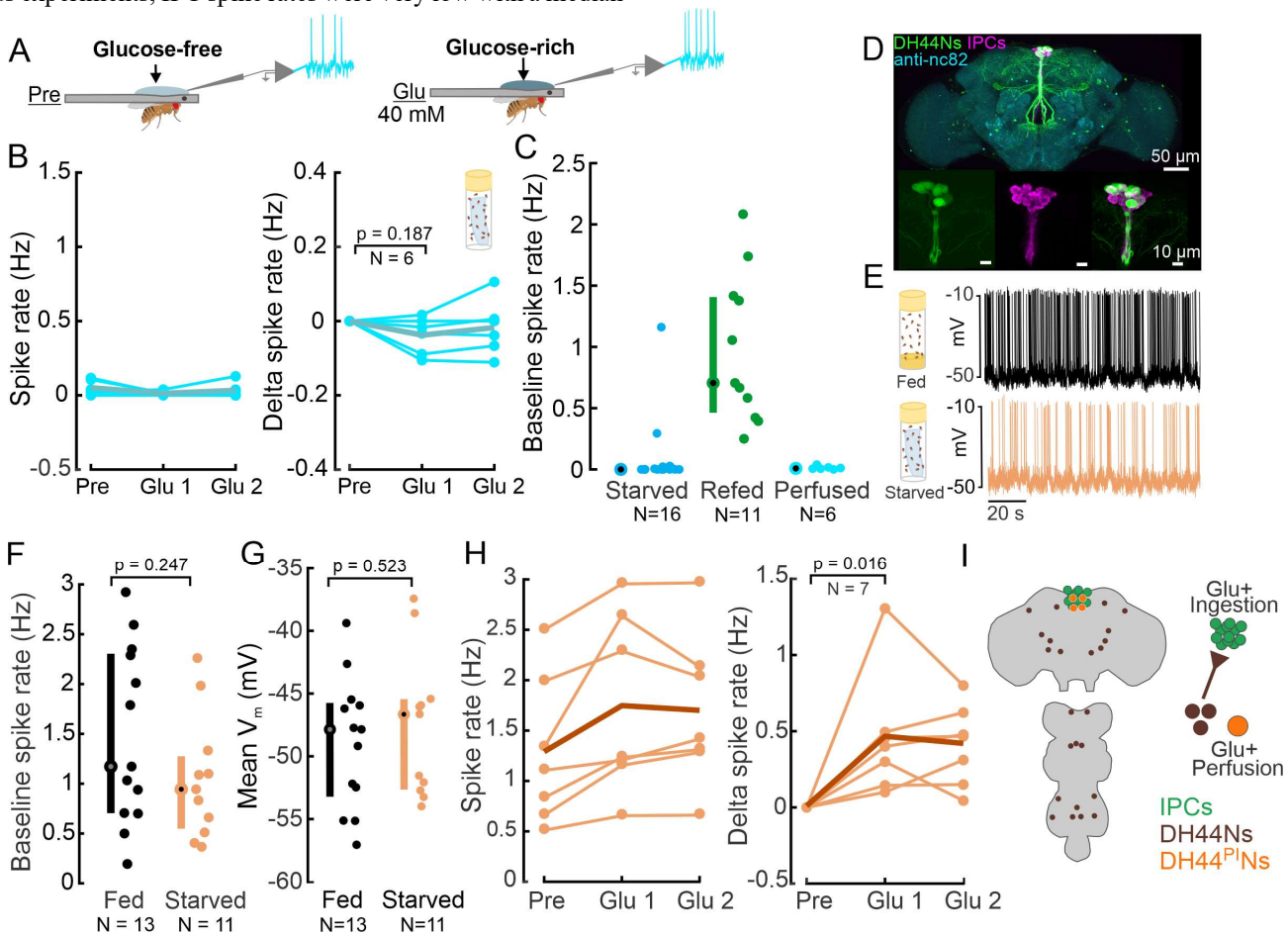

Figure 3: IPCs are not sensitive to glucose perfusion but DH44^{PI}Ns are.
A) Schematic showing the experimental paradigm. IPC and DH44^{PI}N baseline spike rates were recorded in glucose-free extracellular saline followed by recordings in glucose-rich saline. **B)** IPC spike rate and delta spike rate in glucose-free and glucose-rich extracellular saline, in starved flies. Spike rates were averaged within a five minute window. Delta spike rate was calculated by subtracting the baseline (Pre) from each trial for each IPC. Pre: 5-minute recording in glucose-free extracellular saline. Glucose-rich saline was allowed to perfuse for about eight minutes before analyzing IPC activity. Glu1 and Glu2: Two subsequent, 5-minute-long recordings in glucose-rich extracellular saline, starting eight minutes after onset of glucose perfusion. Each circle represents an individual IPC from a different fly, the thick line represents the grand mean of all recordings. p-values were calculated via Wilcoxon signed-rank test. **C)** Comparison of IPC baseline spike rate between starved, glucose-refed, and glucose-perfused flies highlighting the 'incretin effect'. Median and IQR are indicated. **D)** Staining showing *Drosophila* brain with IPCs (magenta) and DH44Ns (green). GFP was enhanced with anti-GFP (green), brain neuropils were stained with anti-nc82 (cyan), and IPCs were labelled using a DILP2 antibody (magenta). **E)** Example membrane potential of a DH44^{PI}N recorded in a fed (black) and a starved fly (orange). **F)** Baseline spike rate in fed (black) and starved flies (orange), each circle represents an individual DH44^{PI}N. **G)** Comparison of the membrane potential of DH44^{PI}Ns in fed and starved flies. Median and IQR are indicated. p-values calculated via Wilcoxon rank-sum test. **H)** Spike rate and delta spike rate of DH44^{PI}Ns in glucose-free and glucose-rich extracellular saline, in starved flies. Thick line represents grand mean. p-value from Wilcoxon signed-rank test. **I)** Schematic showing the regulation of IPCs, DH44^{PI}Ns and DH44Ns outside PI.

of glucose[44,45]. This effect is driven by gut-derived neuropeptides collectively referred to as 'incretin hormones' in mammals[47]. Recently, incretin-like hormones were also described in *Drosophila*[43,66].

DH44^{PI}Ns sense changes in extracellular glucose levels

We were surprised to find that IPCs were not responsive to glucose perfusion and needed to ensure this was not due to shortcomings in our experimental protocol. To validate our approach, we recorded from DH44^{PI}Ns. Dus and co-workers showed that DH44^{PI}Ns are activated by D-glucose via calcium imaging experiments[68]. DH44^{PI}Ns are anatomically similar to IPCs, and their cell bodies are located directly adjacent to those of IPCs in the PI, making them an ideal positive control for our experiments (Figure 3D). When recording from DH44^{PI}Ns *in vivo*, we first observed that their spike amplitude fell within the same range as that of IPCs (Figure 3E, ~40-60 mV). However, DH44^{PI}N baseline spike rates were higher than those of IPCs, ranging from 0.5 Hz to 3 Hz (Figure 3F). Moreover, DH44^{PI}Ns exhibited a firing pattern that was more burst-like (Figure 3E), with much shorter inter-spike-intervals (ISI) than IPCs (Supplementary Figure S3E). When comparing the ISI distribution between DH44^{PI}Ns and IPCs, the fraction of ISIs below 500 ms was 60 % in DH44^{PI}Ns and 19 % in IPCs. The cumulative probability distributions differed significantly (Supplementary Figure S3E, $p << 0.001$). Hence, the two neuron types displayed distinct activity patterns.

Next, we tested the effect of starvation on DH44^{PI}N activity. The baseline spike rate was slightly lower in starved compared to fed flies, but, unlike in IPCs, this difference was not significant (Figure 3F). The membrane potential of DH44^{PI}Ns was also not affected by starvation (Figure 3G). However, the cumulative probability distribution of DH44^{PI}N ISIs differed significantly between starved and fed flies, and ISIs were shifted towards longer durations after starvation ($p << 0.001$, Supplementary Figure S3E). Hence, while the overall spike frequency was unaffected, DH44^{PI}Ns spike patterns were more irregular and burst-like after feeding.

Finally, we tested whether DH44^{PI}Ns are responsive to glucose perfusion. Following the exact same protocol we used for IPC recordings, we perfused the brain with saline containing 40 mM glucose, while patching from DH44^{PI}Ns *in vivo*. The spike rate of DH44^{PI}Ns significantly increased during perfusion with 40 mM glucose in starved flies, by about 0.5 Hz (Figure 3H). The ISI distribution was also significantly shifted towards shorter intervals during glucose perfusion across all flies and within each recording (Supplementary Figure S3F and G). Fed flies, on the other hand, did not exhibit a significant change in DH44^{PI}N activity during glucose perfusion (Supplementary Figure S3D). This indicated that DH44^{PI}Ns are indeed sensitive to glucose perfusion, and that the glucose sensitivity depends on the nutritional state, as previously reported[68]. Together, these experiments reveal two important points: First, DH44^{PI}Ns are glucose sensing, whereas IPCs are not (Figure 3I). Second, the DH44^{PI}N recordings confirm that that our negative result for IPC glucose sensitivity was not an experimental artifact.

DH44Ns outside the PI inhibit IPCs

The proximity of DH44^{PI}N and IPC somata in the same cluster of the PI, their overlapping neurites in the brain (Figure 3D), and the fact that both populations are implicated in metabolic homeostasis prompted us to determine whether these neurons directly interact with each other. To investigate potential functional connectivity between DH44Ns and IPCs, we combined the *UAS-GAL4* and *LexA-LexAop* systems to simultaneously express CsChrimson in all DH44Ns and GFP in IPCs (Figure 4A, see also Supplementary Figure S4A)[27]. This approach enabled us to optogenetically activate DH44Ns while recording from IPCs via patch-clamp.

Optogenetic activation of DH44Ns drove an immediate, strong hyperpolarization of IPCs, which lasted for over one second after stimulus cessation and reduced IPC spiking repeatedly across trials (Figure 4B). This effect was robust across the population of IPCs and flies (Figure 4C). On average, the IPC membrane potential dropped by -5 mV below the baseline during DH44N activation and stayed hyperpolarized until about 1s after activation (Figure 4C). This fast and strong response suggests that DH44Ns could be directly presynaptic to IPCs. To quantify this effect, we calculated the median V_m for each IPC recording in a 500 ms window before the stimulus onset (pre, time windows indicated by grey and colored boxes in Figure 4C) and 200 ms after cessation of the stimulus (post, Figure 4D). All IPCs recorded were strongly hyperpolarized by DH44N activation (Figure 4D, $p = 0.002$). Hence, DH44Ns strongly and significantly inhibited IPCs. Notably, we also recorded from one IPC, which was excited during DH44N activation and inhibited immediately after cessation of activation (Supplementary Figure S4C), indicating heterogeneity in the IPC population[30]. Overall, our results indicate that acute activation of DH44Ns inhibits IPC activity, hence regulating insulin release. This strong inhibition is surprising, since our previous results implicated both, the DH44^{PI}Ns and IPCs, in glucose sensing and metabolic control. Hence, our assumption had been that these modulatory neurons, would display reciprocal excitation rather than inhibition. However, the driver line we used for DH44N activation was relatively broad, and any of the neurons labelled could be responsible for the IPC inhibition. For example, the line labels a subset of DH44Ns ascending from the VNC. A pair of these DH44Ns co-express the neuropeptide Leucokinin (LK)[69], and LK expressing neurons inhibit most IPCs[30].

Therefore, we identified a driver line which only labels the DH44Ns in the PI[70] (*DH44^{PI}–GAL4*) and repeated the functional connectivity experiments using this more specific driver line (Figure 4E, see also Supplementary Figure S4B). Activating exclusively DH44^{PI}Ns had no effect on the IPC membrane potential or spike rate (Figure 4F and, 4G: grand mean remained 0 mV on average). This was consistent across the population of IPCs and flies (Figure 4H, $p = 0.641$). These results confirm that the strong inhibition of IPCs observed when activating the broad DH44N line is not driven by DH44^{PI}Ns. Therefore, DH44^{PI}Ns and IPCs both sense changes in the nutritional state but act independently and in parallel to signal changes in nutritional state (Figure 3I).

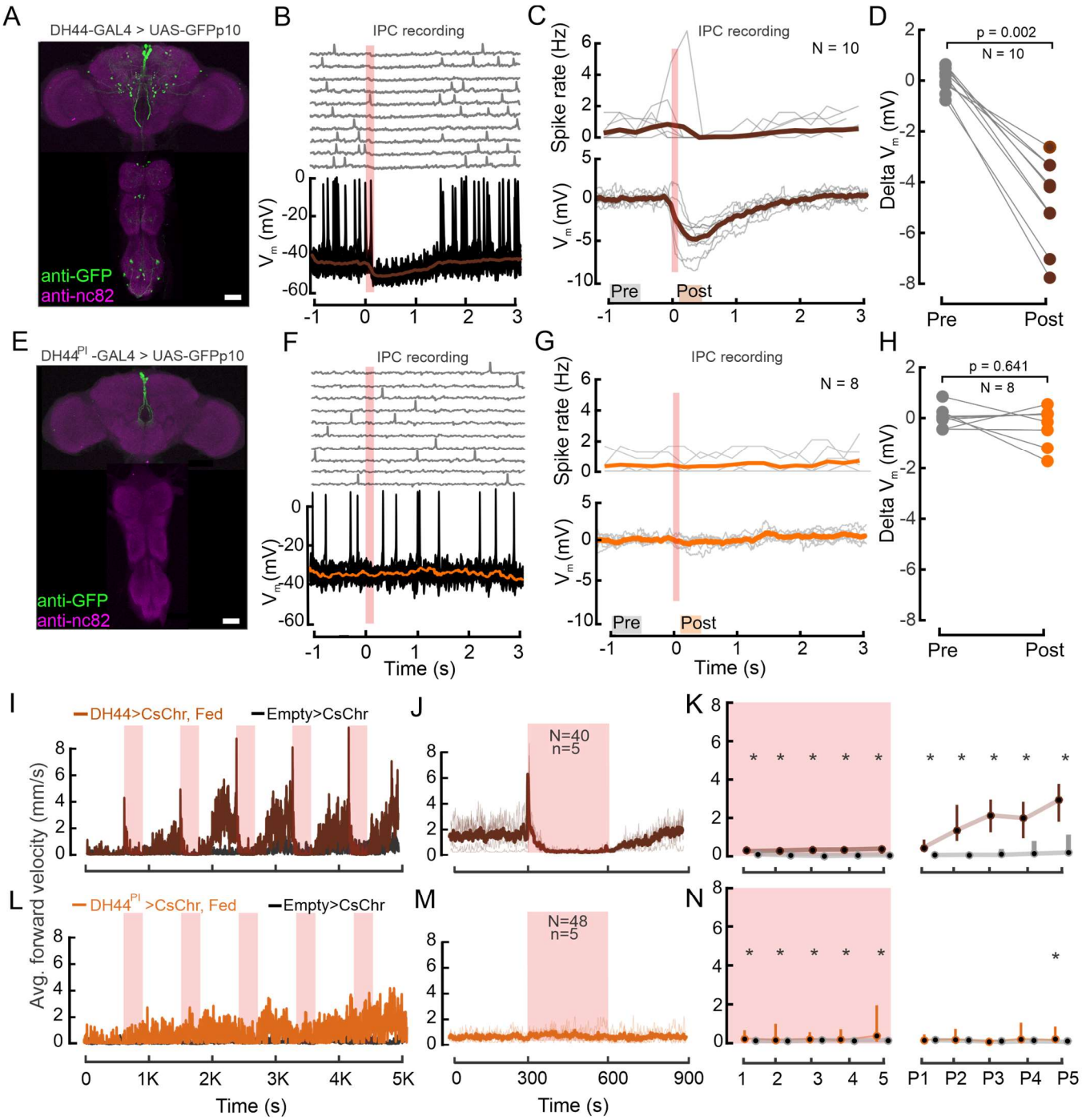

Figure 4: DH44Ns outside the PI inhibit IPCs and drive increases in locomotor activity
A) Immunolabelling showing DH44 expression in the brain and the VNC from broad DH44-GAL4 driver line. GFP was enhanced with anti-GFP (green), brain neuropils were stained with anti-nc82 (magenta) **B)** Example recording of an IPC during optogenetic activation of the DH44Ns (red shading). Upper panel shows individual trials, lower panel shows ten trials overlapped and the median of all trials (brown trace). **C)** Upper panel shows the spike density of individual IPCs across 10 DH44N activations. Lower panel shows the baseline-subtracted, median filtered V_m traces for each IPC. Thick lines represent the grand mean. **D)** Effect of DH44N activation on IPCs. Delta V_m is plotted by calculating the median baseline subtracted V_m from C) 500 ms before (Pre) and 200 ms after DH44N activation (Post). Each circle represents one IPC recording. p-values from Wilcoxon signed-rank test. **E)** Immunolabelling showing GFP expression in the brain and the VNC in the sparse DH44^{PI}-GAL4 driver line. **F)** Example recording of an IPC during optogenetic activation of DH44 neurons using a sparse line which labels only DH44^{PI}Ns. Plot details as in B). **G)** Spike density and baseline subtracted medians of individual IPCs while activating DH44^{PI} line. Plot details as in C). **H)** Pre and post delta V_m of IPCs before and after optogenetic activation of the DH44^{PI} line. Plot details as in in D). **I)** Average FV of 20 flies during optogenetic activation of the DH44Ns using the broad driver line (A). *Empty-GAL4* was used as control for all experiments (black). Red shading shows 300s activation windows. **J)** Average FV across all DH44N activation trials based on two independent replications of the experiment in I. **K)** Average FV of all flies during each stimulus trial (1-5) and post-stimulus trial (300 s window immediately after activation seized, P1-P5). Circles and bars show median and IQR, respectively. Asterisks represent a significant difference according to a Wilcoxon rank-sum test. **L-N)** Behavioral effects of optogenetic DH44^{PI}N activation (see E). Plot details as in I, J and K, respectively. See also Table S3 and S4.

Activation of DH44Ns modulates locomotor activity

Since IPC manipulation had relatively small effects on locomotor activity, other pathways need to be responsible for the strong changes in locomotor activity observed during starvation (Figure 2B). Given their sensitivity for glucose and connectivity to IPCs, DH44Ns were strong candidates. DH44Ns have previously been shown to promote feeding in starved animals[68]. In particular, we hypothesized that the broad DH44N line could have opposite effects to IPCs since a subset of them inhibited IPCs. We therefore tested whether DH44Ns affect locomotor activity by following the same approach as for IPC activation in freely walking flies (Figure 2I-K). Activation of the broad DH44N line resulted in a dramatic increase in FV from a median of 1.8 mm/s to 6 mm/s immediately after light onset (Figure 4I, 4J). This increase was followed by an abrupt halt lasting until the end of the DH44N activation (Figure 4I-K). During this time window of reduced locomotor activity, we observed a strong increase in proboscis extension in 6/20 flies for which we quantified this (Supplementary Figure S4D). The locomotor arrest was released soon after cessation of DH44N activation, upon which locomotor activity increased until the onset of the next stimulation period (Figure 4I and 4K). The FV in the post-activation window increased over subsequent activation cycles and was significantly higher than in controls throughout the experiment (Figure 4I, 4K). The FV of DH44N activated flies increased from a median of 0.3 mm/s to 3 mm/s over five activation cycles, suggesting that long term activation of DH44Ns leads to an increase in locomotion comparable to starvation-induced hyperactivity.

In addition, we tested the driver line labeling only DH44^{PI}Ns. Although we did observe an overall increase in FV of the experimental group, we neither observed an activity peak upon activation onset, nor locomotor arrest during activation (Figure 4L-N). Hence, the strong activation phenotypes were driven by DH44Ns outside the PI. We conclude that the activation of DH44Ns, especially the broad DH44N line, had a pronounced and sustained effect on foraging behavior. The same neurons strongly and significantly inhibited IPCs, suggesting that feeding-promoting and satiety-inducing pathways form inhibitory connections in the CNS as a part of the neuronal mechanisms to ensure reciprocal inhibition of satiety and hunger states.

Discussion

IPC activity is modulated on short and long timescales by the nutritional state, the behavioral state, and aging processes

To advance our understanding of the neuronal underpinnings of metabolic homeostasis, we analyzed the nutritional state-dependent modulation of IPCs in *Drosophila*. Our *in vivo* patch clamp recordings revealed that IPC activity is diminished during starvation and rebounds after glucose feeding. This is consistent with previous studies demonstrating an accumulation of DILPs[26,71–75] and a reduction of *dilp* transcript levels[72,74,75] in IPCs of adult and larval fly brains under starvation and underlines that electrophysiological IPC activity and DILP release are correlated. However, two aspects were surprising about our results. First, the rebound after glucose feeding was relatively slow, and IPC activity built up to baseline levels after over six hours of refeeding. These slow temporal dynamics are a stark contrast to the behavioral state-dependent modulation of IPC activity, which occurs on a timescale of milliseconds[27]. This suggests that IPCs integrate changes in internal states over different timescales and potentially affect metabolism and neuronal networks on both short and long timescales. This idea was further supported by the fact that IPC activity was heavily diminished in flies older than ten days (Supplementary Fig 1B). Reduced insulin signalling has previously been linked to increased life-span in different species, including yeast, worms, flies, and rodents[1]. Our findings demonstrate that IPC activity is significantly reduced both in case of starvation and aging, indicating that insulin release from IPCs is suppressed in these conditions. This suppression of IPC activity could be a mechanism to increase survival under physiologically unfavourable conditions[74]. DILP6 mRNA in the fat body is upregulated during starvation, which has been shown to decrease systemic insulin signaling by the suppression of insulin release from IPCs. This is linked to an increased life-span in *Drosophila*[74]. The second surprising result was that the reduced IPC activity after starvation failed to rebound upon refeeding with high protein and standard diets (Figure 1H). Our standard diet contains glucose at very low concentrations (upper bound of 30 mM, see Methods for details), which explains the lack of an IPC activity rebound. This suggests that starvation had a long-lasting effect on IPC activity, which could specifically be restored by glucose feeding. In addition, insulin signaling might be impaired in flies if they only feed on protein. Similar observations were made in mammals, where prolonged high protein diets lead to insulin resistance and type II diabetes[76,77]. Furthermore, *dilp2* mutants show an increased lifespan[78] which likely results from elevated glycogen phosphorylase activity[79], an enzyme involved in regulating glycogen storage. This suggests that suppressed IPC activity in aged flies could mediate glucose homeostasis by increasing glycogen catabolism. Taken together, the reduced IPC activity we observed in starved and aged flies may be crucial for metabolic adjustments required for survival.

The nutritional state-dependent modulation of IPCs supports the presence of an incretin-like effect in *Drosophila*

Mammalian pancreatic β-cells sense glucose levels in the blood and release insulin accordingly[80,81]. However, this process is much more complex than initially assumed. One key observation is that the ingestion of glucose drives much higher release of insulin compared to the isoglycemic intravenous perfusion of glucose. This difference in insulin release is partially driven by incretin hormones from the gut, for example glucagon-like peptide-1 (GLP-1) and glucose-dependent insulinotropic peptide (GIP)[82–84], which are released after the ingestion of food. Hence, insulin release is modulated by enteroendocrine signals. *Drosophila* IPCs are functionally analogous to mammalian β-cells and presumably sense glucose in the circulating hemolymph to release insulin in response to increases in glucose concentration. Previous *ex vivo* studies suggested that IPCs, like pancreatic β-cells, sense glucose cell-autonomously[23,43]. Consistent with this, we observed an increase in IPC activity after the ingestion of glucose (Fig 2B). However, IPC activity did not increase during the perfusion of glucose directly over the brain. Importantly, the fly preparations were kept alive for several hours allowing the glucose-rich saline to enter circulation and reach all body parts. This suggests that, similar to mammals, IPC activity and hence, insulin release, is not simply modulated by hemolymph glucose concentration in *Drosophila*. Several

pathways could contribute to this. First, although an incretin effect has not been reported in flies before, recent studies provided evidence of incretin-like hormones such as the midgut-derived neuropeptide F in flies[85,86], suggesting that a similar signaling pathway could underlie the incretin effect across species. Second, a subset of IPCs was shown to express the mechanosensitive channel piezo and innervate the crop[87], suggesting that an increase in crop volume during feeding could contribute to the increase in IPC activity after feeding. However, the fact that we observed strong responses of IPCs to glucose intake but not the ingestion of regular food during refeeding suggests this is not the core mechanism underlying the incretin-like effect we observed. Third, taste pathways converge onto IPCs[88] and they could increase IPC activity after the ingestion of glucose via serotonergic inputs from taste responsive cells in the gnathal ganglion. Here, however, we would expect faster responses on the scale of seconds, which are unlikely to shift IPC activity over several hours. Hence, gut-secreted neuropeptides are the strongest candidates to mediate the incretin effect in *Drosophila*. These results signify a causal link between glucose homeostasis in the gut and the brain, and pave the way for further studies investigating the evolutionary conservation of the incretin effect across mammals and insects.

DH44^{PI}Ns and IPCs have distinct, yet interrelated roles in nutrient sensing

Our *in vivo* recordings revealed that IPCs do not sense glucose cell-autonomously, and neither do neurons in the CNS that are directly connected to IPCs – otherwise we would have expected an increase in IPC activity during glucose perfusion. In contrast, DH44^{PI}Ns were sensitive to changes in the extracellular glucose concentration. This could either be driven by cell-autonomous glucose sensitivity or presynaptic glucose sensing neurons. Moreover, DH44^{PI}Ns did not show an increase in activity in fed flies, indicating a lack of sensitivity to glucose ingestion. IPCs responded to glucose ingestion on a timescale of hours, whereas DH44^{PI}Ns immediately responded to increases in extracellular glucose concentrations on a timescale of seconds. These results suggest that DH44^{PI}Ns and IPCs play distinct roles in glucose sensing, which might complement each other. Our initial functional connectivity experiments suggested that the glucose-sensing DH44^{PI}Ns might inhibit IPCs directly. However, refined experiments using a sparse driver line revealed that IPCs are inhibited by DH44Ns outside the PI. If these DH44Ns, like DH44^{PI}Ns, are glucose sensing they would suppress IPC activity in the presence of high glucose concentrations, which would be counteractive. Therefore, even though this remains to be determined, it is likely that these non-PI DH44Ns are activated by signals other than glucose concentrations. Regardless, our results shows that the glucose sensing DH44^{PI}Ns and IPCs act independently of each other. This is coherent with what we established so far: brain DH44^{PI}Ns increase their activity upon glucose sensing.

In line with previous studies[68,89], we found that DH44^{PI}Ns were only activated by glucose in starved flies. Interestingly, this was not because the DH44^{PI}N spike rate was lower after starvation. Instead, DH44^{PI}Ns exhibited similar spike rates in fed and starved flies, but the activity increase in response to glucose perfusion only occurred under starvation. DH44^{PI}Ns also displayed a level of modulation beyond simple increases and decreases in spike frequencies. For example, the ISI distributions of DH44^{PI}Ns were shifted to significantly longer intervals during starvation. This may contribute to the increased glucose sensitivity in starved flies. Moreover, shorter ISIs in fed flies and the more bursty activity pattern could lead to an increase in DH44 peptide release despite similar overall spike frequencies. Apart from this, DH44^{PI}Ns themselves could also become more sensitive to glucose in starved animals. This would suggest that DH44^{PI}Ns sense changes in glucose concentration, rather than the absolute concentration of glucose, in the brain or hemolymph.

Nutritional state-dependent modulation of behavior

Changes in the activity of modulatory neurons affect information processing in neuronal circuits and ultimately behavior[22,54,90–92]. This includes starvation-induced hyperactivity and other aspects of foraging in *Drosophila*. We first tested the causal role of one of the known neuromodulators involved in driving starvation-induced hyperactivity – octopamine. As expected, OAN activation increased locomotor activity, which we interpret as a proxy for foraging based on previous publications[38,93]. The activity levels reached by long-term OAN activation were comparable to the effects of long-term starvation. These results underscore that octopamine plays a major role in driving starvation-induced hyperactivity. Having established the method and approach, we next investigated whether IPCs modulate locomotor activity in flies. This was prompted by the observation that the same parameters that affected IPC activity, i.e., starvation and different diets, also affected the baseline walking activity. However, IPCs only had a minor effect on locomotion. This was despite stimulating IPCs using long, high-intensity optogenetic activation. The strongest effect we observed was a reduction in starvation-induced hyperactivity upon IPC activation, which we interpret as a satiety-like effect due to increased IPC activity. This effect was rather strong in the beginning of the experiment, even before the first activation of IPCs, and was robust across independent repetitions of the same experiment. This effect was likely enhanced by an increased IPC depolarization via CsChrimson activation because of expo sure to visible light during fly handling. However, with subsequent activations, the difference between IPC-activated and control flies was reduced, probably because flies were increasingly food and water-deprived after an hour of activation experiments. In particular the latter could potentially override the reduction in starvation-induced hyperactivity induced by optogenetic IPC activation. Overall, our experiments revealed that IPC activation and resulting insulin release do not lead to a sustained satiety response. This aligns with physiological expectations, as elevated insulin levels exacerbate the glucose deficit in starved flies, which could ultimately lead to increases in hyperactivity via this secondary effect.

Our results also suggest a key role of DH44Ns in modulating aspects of foraging behavior. There is evidence that DH44 release in the brain modulates rest:activity rhythms[94] via downstream targets in the gnathal ganglion[95], which houses circuits involved in the modulation of feeding and locomotion[34,95–100]. Our optogenetic approach provides substantial evidence that DH44Ns drive increased locomotor activity in adult flies, plausibly to enable exploration of the environment for locating food sources. First, the increase in locomotion phenocopies starvation-induced hyperactivity. Second, our experiments additionally showed that DH44Ns outside the PI drive proboscis exten-

sions during stopping, which are one hallmark of feeding behavior. In line with this, a previous study has shown that activation of DH44 receptor 1 neurons, the target neurons of the DH44 neuropeptide, induces proboscis-extension[68]. Both observations suggest that DH44Ns are a component of feeding pathways and mediate nutrient uptake in order to maintain nutritional homeostasis.

Our functional connectivity experiments revealed that these DH44Ns inhibit IPC activity. Initially, promoting feeding and inhibiting insulin release at the same time seems counter-regulatory. However, there are two possible explanations: First, these two effects could be driven by different sub-populations of DH44Ns labelled by the line we used (Fig 4A and E). Second, the IPC inhibition could be part of a combination of physiological effects signaling a hunger state and contribute to the increased foraging activity driven by DH44Ns. Notably, blocking insulin signalling has been reported to mimic starvation in fed flies[54]. Contrary to DH44Ns outside the PI, activation of the glucose-sensing DH44^{PI}Ns did not drive proboscis extension, suggesting that DH44^{PI}Ns are not involved in feeding initiation, but primarily function in post feeding regulation of metabolic homeostasis. This is in line with our electrophysiological results showing that DH44^{PI}N spike frequency is not affected by starvation, and only starts to increase once glucose levels change in the hemolymph. Furthermore, DH44^{PI}N activation increased the FV but did not lead to stopping, suggesting that DH44^{PI}Ns contribute to starvation-induced hyperactivity, whereas other DH44Ns drive stopping.

In conclusion, our study sheds light onto the intricate connections between neuroendocrine signaling, nutrient sensing, and behavior in *Drosophila*. Using electrophysiological approaches, we unraveled the complex activity dynamics of IPCs and DH44^{PI}Ns and identified differences in their activity patterns during various nutritional states. The discovery of an 'incretin-like' effect in flies suggests that important aspects of gut-brain signalling are conserved across vertebrate and invertebrate species. Hence, our findings not only contribute to the increasing body of research on insulin signaling, but also pave the way for future research projects analyzing the intricacies of *Drosophila* neuroendocrine networks governing nutrient sensing.

References

1. Barbieri, M., Bonafè, M., Franceschi, C., and Paolisso, G. (2003). Insulin/IGF-I-signaling pathway: An evolutionarily conserved mechanism of longevity from yeast to humans. Am. J. Physiol. - Endocrinol. Metab. *285*. 10.1152/ajpendo.00296.2003.
2. Brogiolo, W., Stocker, H., Ikeya, T., Rintelen, F., Fernandez, R., and Hafen, E. (2001). An evolutionarily conserved function of the Drosophila insulin receptor and insulin-like peptides in growth control. Curr. Biol. *11*, 213–221. 10.1016/S0960-9822(01)00068-9.
3. Garofalo, R.S. (2002). Genetic analysis of insulin signaling in Drosophila. Trends Endocrinol. Metab. *13*, 156–162. 10.1016/S1043-2760(01)00548-3.
4. Jin Chan, S., and Steiner, D.F. (2000). Insulin Through the Ages: Phylogeny of a Growth Promoting and Metabolic Regulatory Hormone. Integr. Comp. Biol. *40*, 213–222. 10.1093/ICB/40.2.213.
5. Broughton, S.J., Piper, M.D.W., Ikeya, T., Bass, T.M., Jacobson, J., Driege, Y., Martinez, P., Hafen, E., Withers, D.J., Leevers, S.J., et al. (2005). Longer lifespan, altered metabolism, and stress resistance in Drosophila from ablation of cells making insulin-like ligands. Proc. Natl. Acad. Sci. U. S. A. *102*, 3105–3110. 10.1073/pnas.0405775102.
6. Partridge, L., Alic, N., Bjedov, I., and Piper, M.D.W. (2011). Ageing in Drosophila: The role of the insulin/Igf and TOR signalling network. Exp. Gerontol. *46*, 376–381. 10.1016/J.EXGER.2010.09.003.
7. López-Otín, C., Blasco, M.A., Partridge, L., Serrano, M., and Kroemer, G. (2013). The hallmarks of aging. Cell *153*, 1194. 10.1016/J.CELL.2013.05.039.
8. Cahill, G.F. (2006). Fuel Metabolism in Starvation. Annu. Rev. Nutr. 26, 1–22. 10.1146/annurev.nutr.26.061505.111258.
9. Abdul-Ghani, M.A., Tripathy, D., and DeFronzo, R.A. (2006). Contributions of β-Cell Dysfunction and Insulin Resistance to the Pathogenesis of Impaired Glucose Tolerance and Impaired Fasting Glucose. Diabetes Care *29*, 1130–1139. 10.2337/DC05-2179.
10. Carlson, M.G., Snead, W.L., and Campbell, P.J. (1994). Fuel and energy metabolism in fasting humans. Am. J. Clin. Nutr. *60*, 29–36. 10.1093/AJCN/60.1.29.
11. McCue, M.D. (2010). Starvation physiology: Reviewing the different strategies animals use to survive a common challenge. Comp. Biochem. Physiol. Part A Mol. Integr. Physiol. 156, 1–18. 10.1016/j.cbpa.2010.01.002..
12. Finn, P.F., and Dice, J.F. (2006). Proteolytic and lipolytic responses to starvation. Nutrition 22, 830–844. 10.1016/j.nut.2006.04.008.
13. DeFronzo RA. Lilly lecture 1987. The triumvirate: beta-cell, muscle, liver. A collusion responsible for NIDDM. Diabetes. 1988 Jun;37(6):667-87. 10.2337/diab.37.6.667.
14. Hull RL, Westermark GT, Westermark P, Kahn SE (2004). Islet amyloid: a critical entity in the pathogenesis of type 2 diabetes . J Clin Endocrinol Metab. ;89(8):3629-43. 10.1210/jc.2004-0405.
15. Kahn, S.E. (2003). The relative contributions of insulin resistance and beta-cell dysfunction to the pathophysiology of Type 2 diabetes. Diabetologia *46*, 3–19. 10.1007/S00125-002-1009-0.
16. Bellen HJ, Tong C, Tsuda H. 100 years of Drosophila research and its impact on vertebrate neuroscience: a history lesson for the future (2010). Nat Rev Neurosci. ; 11(7):514-22. 10.1038/nrn2839.
17. Baker, K.D., and Thummel, C.S. (2007). Diabetic larvae and obese flies – emerging studies of metabolism in Drosophila. Cell Metab. *6*, 257. 10.1016/J.CMET.2007.09.002.
18. Morris, S.N.S., Coogan, C., Chamseddin, K., Fernandez-Kim, S.O., Kolli, S., Keller, J.N., and Bauer, J.H. (2012). Development of diet-induced insulin resistance in adult Drosophila melanogaster. Biochim. Biophys. Acta - Mol. Basis Dis. *1822*, 1230–1237. 10.1016/j.bbadis.2012.04.012.
19. Chatterjee N, Perrimon N. (2021) What fuels the fly: Energy metabolism in Drosophila and its application to the study of obesity and diabetes. Sci. Adv.7,eabg4336(2021).DOI:10.1126/sciadv.abg4336
20. Park, S., Alfa, R.W., Topper, S.M., Kim, G.E.S., and Kockel, L. (2014). A Genetic Strategy to Measure Circulating Drosophila Insulin Reveals Genes Regulating Insulin Production and Secretion. PLoS Genet *10*, 1004555. 10.1371/journal.pgen.1004555.
21. Jennings, B.H. (2011). Drosophila-a versatile model in biology & medicine. Materials Today;14(5), 190-195. 10.1016/S1369-7021(11)70113-4 10.1016/S1369-7021(11)70113-4..
22. Nässel DR, Winther AM (2010). Drosophila neuropeptides in regulation of physiology and behavior. Prog Neurobiol.;92(1):42-104. doi: 10.1016/j.pneurobio.2010.04.010.
23. Fridell, Y.W.C., Hoh, M., Kréneisz, O., Hosier, S., Chang, C., Scantling, D., Mulkey, D.K., and Helfand, S.L. (2009). Increased uncoupling protein (UCP) activity in Drosophila insulin-producing neurons attenuates insulin signaling and extends lifespan. Aging (Albany. NY). *1*, 699–713. 10.18632/aging.100067.
24. Kim, J., and Neufeld, T.P. (2015). Dietary sugar promotes systemic TOR activation in Drosophila through AKH-dependent selective secretion of Dilp3. Nat. Commun. *6*. 10.1038/ncomms7846.
25. Barber, A.F., Erion, R., Holmes, T.C., and Sehgal, A. (2016). Circadian and feeding cues integrate to drive rhythms of physiology in Drosophila insulin-producing cells. Genes Dev. *30*, 2596–2606. 10.1101/gad.288258.116.
26. Géminard, C., Rulifson, E.J., and Léopold, P. (2009). Remote Control of Insulin Secretion by Fat Cells in Drosophila. Cell Metab. *10*, 199–207. 10.1016/J.CMET.2009.08.002.
27. Liessem, S., Held, M., Bisen, R.S., Haberkern, H., Lacin, H., Bockemühl, T., and Ache, J.M. (2022). Behavioral state-dependent modulation of insulin-producing cells in Drosophila. Curr. Biol. 10.1016/J.CUB.2022.12.005.
28. Luo, J., Lushchak, O. V., Goergen, P., Williams, M.J., and Nässel, D.R. (2014). Drosophila Insulin-Producing Cells Are Differentially Modulated by Serotonin and Octopamine Receptors and Affect Social Behavior. PLoS One *9*, e99732. 10.1371/JOURNAL.PONE.0099732.
29. Barber, A.F., Fong, S.Y., Kolesnik, A., Fetchko, M., and Sehgal, A. (2021). Drosophila clock cells use multiple mechanisms to transmit time-of-day signals in the brain. Proc. Natl. Acad. Sci. U. S. A. *118*, 1–8. 10.1073/pnas.2019826118.

30. Held, M., Bisen, R.S., Zandawala, M., Chockley, A.S., Balles, I.S., Hilpert, S., Liessem, S., Cascino-Milani, F., and Ache, J.M. (2023). Aminergic and peptidergic modulation of Insulin-Producing Cells in Drosophila. bioRxiv, 2023.09.14.557555. 10.1101/2023.09.14.557555.
31. Nässel, D.R., Broeck, J.V. (2016) Insulin/IGF signaling in Drosophila and other insects: factors that regulate production, release and post-release action of the insulin-like peptides. Cell. Mol. Life Sci. 73, 271–290. https://doi.org/10.1007/s00018-015-2063-3
32. Root, C.M., Ko, K.I., Jafari, A., and Wang, J.W. (2011). Presynaptic Facilitation by Neuropeptide Signaling Mediates Odor-Driven Food Search. Cell *145*, 133. 10.1016/J.CELL.2011.02.008.
33. Nässel, D.R., Kubrak, O.I., Liu, Y., Luo, J., and Lushchak, O. V. (2013). Factors that regulate insulin producing cells and their output in drosophila. Front. Physiol. *4*, 252. 10.3389/fphys.2013.00252.
34. Marella, S., Mann, K., and Scott, K. (2012). Dopaminergic Modulation of Sucrose Acceptance Behavior in Drosophila. Neuron *73*, 941–950. 10.1016/J.NEURON.2011.12.032.
35. Pathak, H., and Varghese, J. (2021). Edem1 activity in the fat body regulates insulin signalling and metabolic homeostasis in Drosophila. Life Sci. Alliance 4. 10.26508/LSA.202101079.
36. Ribeiro, C., and Dickson, B.J. (2010). Sex peptide receptor and neuronal TOR/S6K signaling modulate nutrient balancing in Drosophila. Curr. Biol. *20*, 1000–1005. 10.1016/J.CUB.2010.03.061.
37. Brent, A.E., and Rajan, A. (2020). Insulin and Leptin/Upd2 Exert Opposing Influences on Synapse Number in Fat-Sensing Neurons. Cell Metab. *32*, 786-800.e7. 10.1016/j.cmet.2020.08.017.
38. Yang, Z., Yu, Y., Zhang, V., Tian, Y., Qi, W., and Wang, L. (2015). Octopamine mediates starvation-induced hyperactivity in adult Drosophila. Proc. Natl. Acad. Sci. U. S. A. *112*, 5219–5224. 10.1073/PNAS.1417838112.
39. Jourjine, N., Mullaney, B.C., Mann, K., and Scott, K. (2016). Coupled Sensing of Hunger and Thirst Signals Balances Sugar and Water Consumption. Cell *166*, 855–866. 10.1016/J.CELL.2016.06.046.
40. Yu, Y., Huang, R., Ye, J., Zhang, V., Wu, C., Cheng, G., Jia, J., and Wang, L. (2016). Regulation of starvation-induced hyperactivity by insulin and glucagon signaling in adult Drosophila. Elife 5. 10.7554/eLife.15693.001.
41. Enell LE, Kapan N, Söderberg JAE, Kahsai L, Nässel DR (2010) Insulin Signaling, Lifespan and Stress Resistance Are Modulated by Metabotropic GABA Receptors on Insulin Producing Cells in the Brain of Drosophila. PLoS ONE 5(12): e15780. 10.1371/journal.pone.0015780
42. Kapan, N., Lushchak, O. V., Luo, J., and Nässel, D.R. (2012). Identified peptidergic neurons in the Drosophila brain regulate insulin-producing cells, stress responses and metabolism by coexpressed short neuropeptide F and corazonin. Cell. Mol. Life Sci. *69*, 4051–4066. 10.1007/s00018-012-1097-z.
43. Kréneisz, O., Chen, X., Fridell, Y.W.C., and Mulkey, D.K. (2010). Glucose increases activity and Ca2+ in Adult Drosophila Insulin Producing Cells. Neuroreport *21*, 1116. 10.1097/WNR.0B013E3283409200.
44. ELRICK, H., STIMMLER, L., HLAD, C.J., and ARAI, Y. (1964). Plasma Insulin Response to Oral and Intravenous Glucose Administration. J. Clin. Endocrinol. Metab. *24*, 1076–1082. 10.1210/JCEM-24-10-1076.
45. DeFronzo, R.A., Ferrannini, E., Hendler, R., Wahren, J., and Felig, P. (1978). Influence of hyperinsulinemia, hyperglycemia, and the route of glucose administration on splanchnic glucose exchange. *75*, 5173–5177. 10.1073/PNAS.75.10.5173.
46. Creutzfeldt, W. (1979). The incretin concept today. Diabetologia *16*, 75–85. 10.1007/BF01225454/METRICS.
47. Kazafeos, K. (2011). Incretin effect: GLP-1, GIP, DPP4. Diabetes Res. Clin. Pract. *93*, S32–S36. 10.1016/S0168-8227(11)70011-0.
48. Söderberg, J.A.E., Carlsson, M.A., and Nässel, D.R. (2012). Insulin-producing cells in the Drosophila brain also express satiety-inducing cholecystokinin-like peptide, drosulfakinin. Front. Endocrinol. (Lausanne). *3*, 109. 10.3389/FENDO.2012.00109/BIBTEX.
49. Agrawal, N., Delanoue, R., Mauri, A., Basco, D., Pasco, M., Thorens, B., and Léopold, P. (2016). The Drosophila TNF Eiger Is an Adipokine that Acts on Insulin-Producing Cells to Mediate Nutrient Response. Cell Metab. *23*, 675–684. 10.1016/j.cmet.2016.03.003.
50. Lee, G., and Park, J.H. (2004). Hemolymph sugar homeostasis and starvation-induced hyperactivity affected by genetic manipulations of the adipokinetic hormone-encoding gene in Drosophila melanogaster. Genetics *167*, 311. 10.1534/GENETICS.167.1.311.
51. Krashes, M.J., DasGupta, S., Vreede, A., White, B., Armstrong, J.D., and Waddell, S. (2009). A neural circuit mechanism integrating motivational state with memory expression in Drosophila. Cell *139*, 416. 10.1016/J.CELL.2009.08.035.
52. Tsao, C.H., Chen, C.C., Lin, C.H., Yang, H.Y., and Lin, S. (2018). Drosophila mushroom bodies integrate hunger and satiety signals to control innate food-seeking behavior. Elife *7*. 10.7554/ELIFE.35264.
53. Geo, A., Pathak, H., Kujur, A.E., Sudhakar, S., and Kannan, N. (2019). Short Neuropeptide F regulates the starvation mediated enhanced locomotor Activity in Drosophila. 10.1101/764688.
54. Ko, K.I., Root, C.M., Lindsay, S.A., Zaninovich, O.A., Shepherd, A.K., Wasserman, S.A., Kim, S.M., and Wang, J.W. (2015). Starvation promotes concerted modulation of appetitive olfactory behavior via parallel neuromodulatory circuits. Elife *4*. 10.7554/ELIFE.08298.
55. Chockley, A.S., Dinges, G.F., Di Cristina, G., Ratican, S., Bockemühl, T., and Büschges, A. (2022). Subsets of leg proprioceptors influence leg kinematics but not interleg coordination in Drosophila melanogaster walking. J. Exp. Biol. *225*. 10.1242/JEB.244245.
56. Eyjolfsdottir, E., Branson, S., Burgos-Artizzu, X.P., Hoopfer, E.D., Schor, J., Anderson, D.J., and Perona, P. (2014). Detecting social actions of fruit flies. Lect. Notes Comput. Sci. (including Subser. Lect. Notes Artif. Intell. Lect. Notes Bioinformatics) *8690 LNCS*, 772–787.
57. Brembs, B., Christiansen, F., Pflüger, H.J., and Duch, C. (2007). Flight Initiation and Maintenance Deficits in Flies with Genetically Altered Biogenic Amine Levels. J. Neurosci. *27*, 11122. 10.1523/JNEUROSCI.2704-07.2007.
58. Suver, M.P., Mamiya, A., and Dickinson, M.H. (2012). Octopamine neurons mediate flight-induced modulation of visual processing in Drosophila. Curr. Biol. *22*, 2294–2302. 10.1016/J.CUB.2012.10.034.
59. Klapoetke, N.C., Murata, Y., Kim, S.S., Pulver, S.R., Birdsey-Benson, A., Cho, Y.K., Morimoto, T.K., Chuong, A.S., Carpenter, E.J., Tian, Z., et al. (2014). Independent Optical Excitation of Distinct Neural Populations. Nat. Methods *11*, 338. 10.1038/NMETH.2836.
60. Monastirioti, M., Linn, C.E., and White, K. (1996). Characterization of Drosophila Tyramine β-HydroxylaseGene and Isolation of Mutant Flies Lacking Octopamine. J. Neurosci. *16*, 3900. 10.1523/JNEUROSCI.16-12-03900.1996.
61. Hampel, S., Franconville, R., Simpson, J.H., and Seeds, A.M. (2015). A neural command circuit for grooming movement control. Elife *4*. 10.7554/ELIFE.08758.
62. Sayin, S., De Backer, J.F., Siju, K.P., Wosniack, M.E., Lewis, L.P., Frisch, L.M., Gansen, B., Schlegel, P., Edmondson-Stait, A., Sharifi, N., et al. (2019). A Neural Circuit Arbitrates between Persistence and Withdrawal in Hungry Drosophila. Neuron *104*, 544-558.e6. 10.1016/J.NEURON.2019.07.028.
63. Saraswati, S., Fox, L.E., Soll, D.R., and Wu, C.F. (2004). Tyramine and Octopamine Have Opposite Effects on the Locomotion of Drosophila Larvae. J. Neurobiol. *58*, 425–441. 10.1002/NEU.10298.
64. Selcho, M., Pauls, D., el Jundi, B., Stocker, R.F., and Thum, A.S. (2012). The Role of octopamine and tyramine in Drosophila larval locomotion. J. Comp. Neurol. *520*, 3764–3785. 10.1002/CNE.23152.
65. Ormerod, K.G., Hadden, J.K., Deady, L.D., Mercier, A.J., and Krans, J.L. (2013). Action of octopamine and tyramine on muscles of Drosophila melanogaster larvae. J. Neurophysiol. *110*, 1984–1996. 10.1152/JN.00431.2013.
66. Fox, L.E., Soll, D.R., and Wu, C.-F. (2006). Coordination and modulation of locomotion pattern generators in Drosophila larvae: effects of altered biogenic amine levels by the tyramine beta hydroxlyase mutation. J. Neurosci. Off. J. Soc. Neurosci. *26*, 1486–1498. 10.1523/JNEUROSCI.4749-05.2006.
67. Kréneisz, O., Chen, X., Fridell, Y.W.C., and Mulkey, D.K. (2010). Glucose increases activity and Ca2+ in insulin-producing cells of adult Drosophila. Neuroreport *21*, 1116–1120. 10.1097/WNR.0b013e3283409200.
68. Dus, M., Lai, J.S.Y., Gunapala, K.M., Min, S., Tayler, T.D., Hergarden, A.C., Geraud, E., Joseph, C.M., and Suh, G.S.B. (2015). Nutrient Sensor in the Brain Directs the Action of the Brain-Gut Axis in Drosophila. Neuron *87*, 139–151. 10.1016/j.neuron.2015.05.032.
69. Zandawala, M., Marley, R., Davies, S.A., and Nässel, D.R. (2018). Characterization of a set of abdominal neuroendocrine cells that regulate stress physiology using colocalized diuretic peptides in Drosophila. Cell. Mol. Life Sci. *75*, 1099–1115. 10.1007/S00018-017-2682-Y/TABLES/4.
70. Asahina, K., and Anderson, D. (2013). Neuropeptide-GAL4 constructs and insertions.
71. Colombani, J., Raisin, S., Pantalacci, S., Radimerski, T., Montagne, J., and Léopold, P. (2003). A nutrient sensor mechanism controls Drosophila growth. Cell *114*, 739–749. 10.1016/S0092-8674(03)00713-X.
72. Ikeya, T., Galic, M., Belawat, P., Nairz, K., and Hafen, E. (2002). Nutrient-dependent expression of insulin-like peptides from neuroendocrine cells in the CNS contributes to growth regulation in Drosophila. Curr. Biol. *12*, 1293–1300. 10.1016/S0960-9822(02)01043-6.

73. Rajan, A., and Perrimon, N. (2012). Drosophila Cytokine Unpaired 2 Regulates Physiological Homeostasis by Remotely Controlling Insulin Secretion. Cell *151*, 123–137. 10.1016/J.CELL.2012.08.019.
74. Bai, H., Kang, P., and Tatar, M. (2012). Drosophila insulin-like peptide-6 (dilp6) expression from fat body extends lifespan and represses secretion of Drosophila insulin-like peptide-2 from the brain. Aging Cell *11*. 10.1111/acel.12000.
75. Sudhakar, S.R., Pathak, H., Rehman, N., Fernandes, J., Vishnu, S., and Varghese, J. (2020). Insulin signalling elicits hunger-induced feeding in Drosophila. Dev. Biol. *459*, 87–99. 10.1016/J.YDBIO.2019.11.013.
76. Claessens, M., Saris, W.H.M., and Van Baak, M.A. (2008). Glucagon and insulin responses after ingestion of different amounts of intact and hydrolysed proteins. Br. J. Nutr. *100*, 61–69. 10.1017/S0007114507886314.
77. Rietman, A., Schwarz, J., Tomé, D., Kok, F.J., and Mensink, M. (2014). High dietary protein intake, reducing or eliciting insulin resistance? Eur. J. Clin. Nutr. 2014 689 *68*, 973–979. 10.1038/ejcn.2014.123.
78. Grönke, S., Clarke, D.F., Broughton, S., Andrews, T.D., and Partridge, L. (2010). Molecular Evolution and Functional Characterization of Drosophila Insulin-Like Peptides. PLoS Genet. *6*, 1000857. 10.1371/JOURNAL.PGEN.1000857.
79. Post, S., Karashchuk, G., Wade, J.D., Sajid, W., De Meyts, P., and Tatar, M. (2018). Drosophila insulin-like peptides DILP2 and DILP5 differentially stimulate cell signaling and glycogen phosphorylase to regulate longevity. Front. Endocrinol. (Lausanne). *9*, 1–16. 10.3389/fendo.2018.00245.
80. Matschinsky, F.M. (1996). Banting Lecture 1995. A lesson in metabolic regulation inspired by the glucokinase glucose sensor paradigm. Diabetes *45*, 223–241. 10.2337/DIAB.45.2.223.
81. MacDonald, P.E., Joseph, J.W., and Rorsman, P. (2005). Glucose-sensing mechanisms in pancreatic -cells. Philos. Trans. R. Soc. B Biol. Sci. *360*, 2211–2225. 10.1098/RSTB.2005.1762.
82. Buchan, A.M., Polak, J.M., Capella, C., Solcia, E., and Pearse, A.G. (1978). Electronimmunocytochemical evidence for the K cell localization of gastric inhibitory polypeptide (GIP) in man. Histochemistry *56*, 37–44. 10.1007/BF00492251.
83. Meier, J.J., Nauck, M.A., Schmidt, W.E., and Gallwitz, B. (2002). Gastric Inhibitory Polypeptide: the neglected incretin revisited. Regul. Pept. *107*, 1–13. 10.1016/S0167-0115(02)00039-3.
84. Brown, J.C. (1982). Gastric inhibitory polypeptide. Monogr. Endocrinol. *24*, III–XI, 1–88.
85. Yoshinari, Y., Kosakamoto, H., Kamiyama, T., Hoshino, R., Matsuoka, R., Kondo, S., Tanimoto, H., Nakamura, A., Obata, F., and Niwa, R. (2021). The sugar-responsive enteroendocrine neuropeptide F regulates lipid metabolism through glucagon-like and insulin-like hormones in Drosophila melanogaster. Nat. Commun. 2021 121 *12*, 1–21. 10.1038/s41467-021-25146-w.
86. Malita, A., Kubrak, O., Koyama, T., Ahrentløv, N., Texada, M.J., Nagy, S., Halberg, K. V., and Rewitz, K. (2022). A gut-derived hormone suppresses sugar appetite and regulates food choice in Drosophila. Nat. Metab. 2022 411 *4*, 1532–1550. 10.1038/s42255-022-00672-z.
87. Wang, P., Jia, Y., Liu, T., Jan, Y.N., and Zhang, W. (2020). Visceral Mechano-sensing Neurons Control Drosophila Feeding by Using Piezo as a Sensor. Neuron *108*, 640-650.e4. 10.1016/j.neuron.2020.08.017.
88. Yao, Z., and Scott, K. (2022). Serotonergic neurons translate taste detection into internal nutrient regulation. Neuron *110*, 1036-1050.e7. 10.1016/j.neuron.2021.12.028.
89. Oh, Y., Lai, J.S.Y., Mills, H.J., Erdjument-Bromage, H., Giammarinaro, B., Saadipour, K., Wang, J.G., Abu, F., Neubert, T.A., and Suh, G.S.B. (2019). A glucose-sensing neuron pair regulates insulin and glucagon in Drosophila. Nat. 2019 5747779 *574*, 559–564. 10.1038/s41586-019-1675-4.
90. Marder, E. (2012). NEUROMODULATION OF NEURONAL CIRCUITS: BACK TO THE FUTURE. Neuron *76*, 1. 10.1016/J.NEURON.2012.09.010.
91. van den Pol, A.N. (2012). Neuropeptide transmission in brain circuits. Neuron *76*, 98–115. 10.1016/J.NEURON.2012.09.014.
92. Asahina, K., Watanabe, K., Duistermars, B.J., Hoopfer, E., González, C.R., Eyjólfsdóttir, E.A., Perona, P., and Anderson, D.J. (2014). Tachykinin-expressing neurons control male-specific aggressive arousal in Drosophila. Cell *156*, 221–235. 10.1016/J.CELL.2013.11.045.
93. Huang, R., Song, T., Su, H., Lai, Z., Qin, W., Tian, Y., Dong, X., and Wang, L. (2020). High-fat diet enhances starvation-induced hyperactivity via sensitizing hunger-sensing neurons in drosophila. Elife *9*, 1–26. 10.7554/eLife.53103.
94. Cavanaugh, D.J., Geratowski, J.D., Wooltorton, J.R.A., Spaethling, J.M., Hector, C.E., Zheng, X., Johnson, E.C., Eberwine, J.H., and Sehgal, A. (2014). Identification of a Circadian Output Circuit for Rest:Activity Rhythms in Drosophila. Cell *157*, 689–701. 10.1016/J.CELL.2014.02.024.
95. King, A.N., Barber, A.F., Smith, A.E., Dreyer, A.P., Sitaraman, D., Nitabach, M.N., Cavanaugh, D.J., and Sehgal, A. (2017). A Peptidergic Circuit Links the Circadian Clock to Locomotor Activity. Curr. Biol. *27*, 1915-1927.e5. 10.1016/J.CUB.2017.05.089.
96. Singh, R.N. (1997). Neurobiology of the gustatory systems of Drosophila and some terrestrial insects. Microsc. Res. Tech. *39*, 547–563. 10.1002/(SICI)1097-0029(19971215)39:6<547::AID-JEMT7>3.0.CO;2-A.
97. Sterne, G.R., Otsuna, H., Dickson, B.J., and Scott, K. (2021). Classification and genetic targeting of cell types in the primary taste and premotor center of the adult Drosophila brain. Elife *10*.
98. Colomb, J., Grillenzoni, N., Ramaekers, A., and Stocker, R.F. (2007). Architecture of the primary taste center of Drosophila melanogaster larvae. J. Comp. Neurol. *502*, 834–847. 10.1002/cne.21312.
99. Tastekin, I., Riedl, J., Schilling-Kurz, V., Gomez-Marin, A., Truman, J.W., and Louis, M. (2015). Role of the Subesophageal Zone in Sensorimotor Control of Orientation in Drosophila Larva. Curr. Biol. *25*, 1448–1460. 10.1016/J.CUB.2015.04.016.
100. Cobb M, Scott K, Pankratz M. (2009). Gustation in Drosophila melanogaster. SEB Exp Biol Ser. 63:1-38.
101. Wagh, D.A., Rasse, T.M., Asan, E., Hofbauer, A., Schwenkert, I., Durrbeck, H., Buchner, S., Dabauvalle, M.C., Schmidt, M., Qin, G., et al. (2006). Bruchpilot, a protein with homology to ELKS/CAST, is required for structural integrity and function of synaptic active zones in Drosophila. Neuron *49*, 833-844.
102. Schindelin, J., Arganda-Carreras, I., Frise, E., Kaynig, V., Longair, M., Pietzsch, T., … Cardona, A. (2012). Fiji: an open-source platform for biological-image analysis. *Nature Methods*, *9*(7), 676–682.10.1038/nmeth.2019

Author contributions

Writing – original draft, R.S.B. and J.M.A.; writing – review & editing, R.S.B., T.B. and J.M.A.; patch-clamp recordings, R.S.B.; behavioral experiments, F.M.I., anatomy, R.S.B; software, F.C.-M., T. B. and J.M.A.; formal analysis, R.S.B., F.M.I., F.C.-M.; supervision, J.M.A.; project conceptualization, R.S.B. and J.M.A; project administration, J.M.A; funding acquisition, J.M.A.

.

Acknowledgements

We thank Haluk Lacin (University of Missouri-Kansas City) who provided fly lines for activation experiments and Jan A. Veenstra (University of Bordeaux) for sharing the DILP2 antibody. We thank Konrad Öchsner for technical assistance and Charlotte Helfrich-Förster and Wolfgang Rössler (all Julius-Maximilians-Universität of Würzburg) for sharing resources. We are also thankful to Christian Wegener and Meet Zandawala (both JMU) for helpful discussions. Tanja A. Godenschwege (Florida Atlantic University), Chris J. Dallmann, Sander Liessem, and Martina Held (all JMU) shared valuable feedback on the manuscript. This work was supported by a grant from the Deutsche Forschungsgemeinschaft (DFG) to J.M.A. via the Emmy Noether program (DFG AC 371/1-1), and by a grant from the DFG to J.M.A. as part of the NSF/CIHR/DFG/FRQ/UKRI-MRC Next Generation Networks for Neuroscience (Neuronex) Program (DFG AC 371/2-1).

Competing interest statement

The authors declare no competing interests, financial or otherwise.

Materials and Methods

Fly husbandry

The following fly strains were used: *DILP2-GAL4; CyO* (BDSC #37516), *10XUAS-IVS-myr::GFP* (BDSC #32197), *TDC2-GAL4* (#BDSC 9313), *DH44-GAL4* (BDSC #39347), *DH44^{PI}-GAL4* (BDSC #51987), *R96A08-LexA-p65-vk37::LexOp-dilp2::GFP; 20x-UAS-CsChrimson-attp2/ TM6b* (as described in Liessem et al., 2023) 10X*UAS-GFP-P10* (BDSC #32201), *20x-UAS-CsChrimson* (BDSC #55134), *Empty split-GAL4* (BDSC #86738). *DILP2-GAL4* and *DH44-GAL4* driver lines were crossed with *10XUAS-IVS-myr::GFP* to drive the expression of GFP in IPCs and DH44Ns, respectively. For electrophysiology combined with optogenetics, DH44N driver lines were crossed with *R96A08-LexA-p65-vk37::LexOp-dilp2::GFP; 20x-UAS-CsChrimson-attp2/TM6b*, hence expressing CsChrimson in DH44Ns and GFP in IPCs.

Flies were raised at 25°C and 60% humidity under a 12h/12h light/dark cycle, on standard fly food containing per liter: 147.5 g cornmeal, 10 g soy flour, 18.5 g Cenovis (beer yeast), 6.25 g agar-agar, 45 g malt syrup, 45 g sugar beet molasses, and 2.5 g Nipagin. For starvation, flies were kept in

empty vials with a filter paper soaked in water. For refeeding experiments, starved flies were refed on 2 % agar with either 400 mM glucose (high glucose diet) or 10 % yeast extract (high protein diet) or standard fly food (standard diet). For optogenetic experiments, 300 µM of all-trans-retinal (R2500, Sigma-Aldrich, Steinheim, Germany) was added to 10 ml of fly food. These vials were kept in darkness until the flies were used for experiments.

Our standard lab diet does not contain glucose as such, but we estimated the concentration of glucose based on indirect sources of glucose (malt syrup and sugar beet molasses). Based on the percentage of glucose present in malt syrup (7%) and sugar beet molasses (4.55 g per 100 g), we estimate that our lab diet contains about 28.4 mM glucose.

Electrophysiology

All experiments were performed in mated females between 3-6 days post eclosion, except for comparison of IPC activity between different age groups and mating states. Flies were cold anesthetized on ice and then immobilized in a custom-made shim plate fly holder using UV glue (Proformic C1001, VIKO UG, Munich, Germany). The proboscis was glued to the thorax to restrict brain movement, and the front legs were excised. The cuticle was then removed in a window above the pars intercerebralis so that the posterior-dorsal part of the fly brain was exposed. Trachea and the ocellar ganglion were removed to render the IPCs accessible. The fly was then transferred with the fly holder into a customized, upright fluorescence microscope setup (Olympus BX51WIF, Evident Corporation, Japan). Live images of the fly brain were acquired with a high-resolution camera (SciCam Pro, Scientifica, US) using an image acquisition software (OCULAR™, Digital Optics Limited, Auckland, NZ). During the preparation, as well as the experiment, the brain was continuously perfused with carbonated (95% O2 and 5% CO2) extracellular saline containing, 103 mM NaCl, 3 mM KCl, 5 mM N-[Tris(hydroxymethyl)methyl]-2-aminoethanesulfonic acid, 20 mM sucrose, 26 mM NaHCO3, 1 mM NaH2PO4, 1.5 mM CaCl2.2H2O, 4 mM MgCl2.6H2O, and osmolarity adjusted to 273-275 mOsm (modified from Gouwens & Wilson, 2009). 0.025% Collagenase (w/v in extracellular saline, Sigma-Aldrich #C5138) was gently applied using a thin-walled glass pipette, to dissociate the neural sheath above IPCs. IPC cell bodies were identified via GFP expression and whole-cell patch clamp recordings were performed using thick-walled patch pipettes (4 – 8 MΩ resistance) containing intracellular saline (40 mM potassium aspartate, 10 mM HEPES, 1 mM EGTA, 4 mM MgATP, 0.5 mM Na3 GTP, 1 mM KCl and 20 µM, adjusted to 260–275 mOsm, pH 7.3). Continuous time series of the membrane potential and spike events were captured in current clamp mode with an AxoPatch MultiClamp 200B (Molecular Devices, Sunnydale, CA) and corrected for a 13 mV liquid junction potential (Gouwens and Wilson, 2009). All data were recorded with a Digidata 1440A analog-digital converter (Molecular Devices), controlled by the pCLAMP 10 software using a 10 kHz low-pass filter and a 20 kHz sampling rate. Recordings were accepted for analysis if the resting membrane potential was < -48 mV and the spike amplitude > 20 mV.

For glucose perfusion experiments. IPC activity was recorded in glucose-free extracellular saline for 10 minutes to establish the baseline. Next, the brain was perfused with extracellular saline replacing sucrose with 40 mM. The switch between the salines took about three minutes, when the glucose-rich saline reached the brain. The membrane potential in glucose-rich saline was then recorded for 15 minutes in three consecutive five-minute recordings. Out of these, the last two recordings (Glu1 and Glu2) were used for analysis in order to make sure that glucose has perfused into the brain.

For optogenetic experiments during electrophysiological recordings, CsChrimson was activated using a 625 nm LED with an intensity adjusted to ~4.4mW/cm^2 at the position of the fly. The activation protocol was triggered by the pCLAMP software. Each recording consisted of 10 activations with the LED ON for 100 ms, interleaved with a 10 s long inter-stimulus-interval. TTL triggers were used to drive the LED and were recorded simultaneously with intracellular traces in the abf format (Axon Binary File).

Quantification and statistical analysis for electrophysiology

All data analysis was performed in MATLAB R2021a (The Mathworks, Natick, MA). The statistical tests we used and p-values are mentioned in the figure legends and captions. All data points are presented with median and interquartile ranges.

Intracellular recordings were temporally smoothed using the *smooth* function in MATLAB and the 'loess' method with span 7. Spike thresholds were set manually in either the recording or the derivative of the recording to detect spikes. Accurate spike detection was monitored manually. For the analysis of changes in membrane potential (V_m), the median of intracellular traces was used. Spike density of individual neurons across the 10 different trials of the short stimulation protocol, was computed by using 250 ms time bins across 10 activation trials.

Immunohistochemistry and image acquisition

For immunolabelling, respective driver lines were crossed with a *UAS-GFP-P10* reporter to endogenously express cytosolic GFP in the neurons of interest. Flies were anesthetized on ice and then transferred to 1.5 ml 4% paraformaldehyde in 0.1 M phosphate buffer saline containing 0.5% Triton- X100 (PBT). The flies were fixed in this solution for 3-6 hours over a digital rotator (IKA Loopster digital) followed by three 15 minutes wash steps in PBT. Individual fly brains were then dissected in a SYLGARD® dish after immersing the fly briefly in 70 % ethanol. Dissected brains were then washed three times in PBT for 15 minutes followed by blocking in 10% normal goat serum in 0.1 M PBT (blocking buffer), for either 2 hours at room temperature or overnight at 4 °C. Next, the samples were incubated for 2 days at 4°C in primary antibody solutions in blocking buffer. We used rabbit anti-DILP2 diluted to 1:2000 (RRID: AB_2569969, kindly provided by J. A. Veenstra, Bordeaux, France) to label IPCs, mouse anti-nc82 (Bruchpilot C-terminal aa 1227-1740)[101] diluted as 1:500 to label the neuropils as background, and chicken anti-GFP (ab13970, abcam, Berlin, Germany) diluted to 1:1000 to enhance the endogenous GFP signal. Afterwards, brains were washed in PBT for three consecutive 15 minutes washes, followed by overnight incubation in secondary antibody solutions at 4°C in the dark. Here, we used AlexaFluor-488 (goat anti-chicken IgY (H+L), Thermo Fisher Scientific, Waltham, MA, USA) diluted to 1:200, AlexaFluor 635 (goat anti-mouse IgG (H+L), Thermo Fisher Scientific) diluted to 1:400, and AlexaFluor 555 (goat anti-rabbit IgG (H+L), Thermo Fisher Scientific) diluted to 1:200. Finally, samples were washed thrice again in PBT before mounting them in Vectashield Antifade Mounting Medium (H-1000, Vector Laboratories, CA, USA).

Image acquisition was performed with a confocal laser-scanning microscope (Leica TCS SP8 WLL) through the Leica Application Suite (LAS X, Leica Microsystems, Wetzlar, Germany) using HC PL APO 10×/0.4, HC PL APO 20×/0.75 IMM, or HC PL APO 63×/1.2 CORR objectives. Fluorescence was detected using suitable lasers with a resolution of 1024 x 1024 pixels, in serial stacks. Final image processing to adjust contrast and brightness was done in Fiji[102].

Survival assay

For conducting a survival assay, two replicates of 20 flies per condition were used. Initially, 3-4 days old adult female flies were wet-starved for 24 hours, and then refed on either HG, HP, or SD. They were kept on these diets for the rest of their survival span and were transferred onto fresh food every second day. The number of survivors was counted once each day and dead flies were removed. For analysis of survival percentage, we summed the values across two replicates.

Free-walking assay

The pre-processed single-nucleus transcriptome data for IPCs was downloaded from https://www.flycellatlas.org/ (Li et al., 2022). This data was further processed and analyzed with the Seurat package (version 4.1.1; https://satijalab.org/seurat/articles/pbmc3k_tutorial.html) in R-Studio (Hao et al., 2021). The original data comprised of 658 single cell transcriptomes, derived from 250 males and 250 females, and sequenced using the Smart-seq2 technology. We used a stringent criterion (*Ilp2* > 0 & *Ilp3* > 0 & *Ilp5* > 0) to retrieve 392 IPC transcriptomes (from 194 male and 198 female flies transcriptomes) which express all three *Ilps*. Standard commands in Seurat were used to perform the t-distributed Stochastic Neighbor Embedding (t-SNE) analysis and create dot plots and feature plots. Heatmaps were generated using the heatmap package (1.0.12).

Virgin female flies carrying *20x-UAS-Cs-Chrimson-m-venus*[59] were mated with males from the neuromodulatory GAL4 lines studied. Post eclosion, the offspring was reared on standard food coated with 300 µM all-trans retinal for a period of three to six days prior to the experiment. In the experiments that involved starved flies, flies were transferred to a plastic vial containing a small piece of wet tissue paper for 24 h before the start of the experiment. The walking activity of up to 20 flies was recorded using the 'Universal Fly Observatory' (UFO) behavioral setup which is based on an earlier study[55]. The UFO features a walking arena consisting of an inverted petri dish of diameter 100 mm as its base. To prevent escape, this base was covered with a watch glass of diameter 120 mm. The inside of the watch glass was coated with SigmaCote siliconizing reagent (cat. no. SL2; Sigma-Aldrich, RRID: SCR_008988) to prevent flies from walking upside down on the watch glass. The arena was illuminated by a ring of 60 infrared (IR) LEDs (wavelength: 870 nm) arranged concentrically around the arena. A diffuser was placed along the inner side of IR LED ring to ensure uniform illumination across the entire arena. The arena was filmed from below via a surface mirror positioned at a 45° angle below the arena and a camera (Basler acA1300-200um, Basler AG, Ahrensburg, Germany) with a spatial resolution of 0.08 mm/pixel and a temporal resolution of 20 Hz. The camera's lens was equipped with an IR-pass filter (lower cut-off frequency: 760nm) that only permits the IR light to pass through to ensure a strong contrast between the

background (black) and the flies (bright). A second ring of 60 red LEDs (wavelength: 625 nm) positioned above the IR LED ring provided the light necessary to transiently activate CsChrimson for optogenetic activation. The entire UFO setup was enclosed within a box, together with a second UFO, which includes a visible white light source placed above the arena for controlled light conditions.

Before each experiment, twenty flies were transferred to an empty vial and anesthetized on ice for two minutes. Subsequently, flies were transferred to the UFO arena. They were given a recovery period of ten minutes to explore the arena before starting the experiment. One complete experiment consisted of five activation cycles and each activation cycle lasted 15 minutes and included 5 minutes of exposure to red light, for a total duration of 90 minutes per experiment. All experiments were conducted under white light conditions. For each neuromodulator line, the experimental flies and control flies were recorded simultaneously in two separate UFOs situated in the same enclosure. Both the protocol and video acquisition were controlled with custom-written MATLAB code.

Movement of flies was tracked using the Caltech Fly Tracker software[56]. A detailed description of the tracking software is available at https://kristinbranson.github.io/FlyTracker/index.html. The position of individual flies was extracted from the videos on a frame by frame basis and features like translational and angular velocity were further computed in MATLAB. We excluded flies that died during the experiments from the tracking dataset prior to analysis. Additionally, we ensured that no identity switches occurred to dead flies throughout the experiment. We conducted a minimum of 2 replicates for each experimental line and its corresponding controls and combined their tracking data for analysis. For plotting the average velocity across all flies, we implemented a data down-sampling by a factor of 20. Statistical analysis was conducted using MATLAB with the Wilcoxon rank-sum test.

Supplementary material

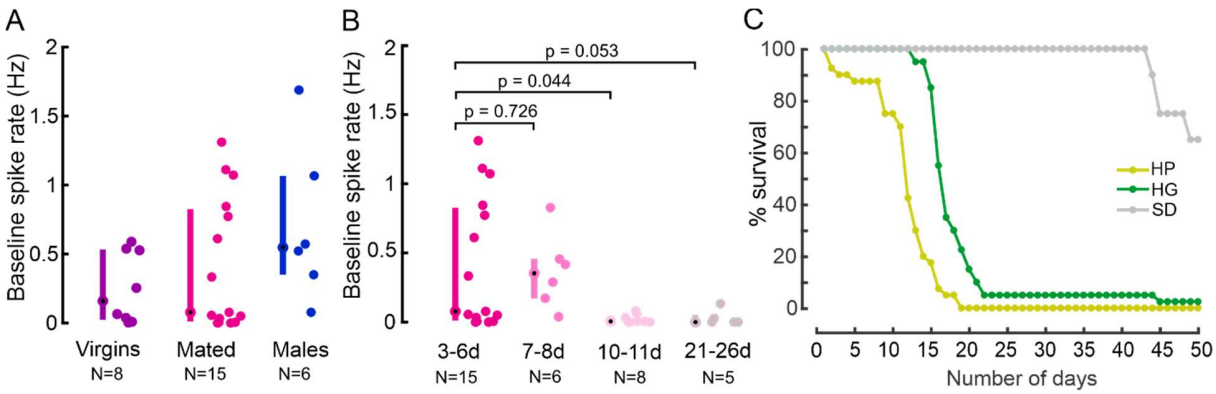

Figure S1: Mating state and aging affect IPC activity, and dietary restriction impairs survival in *Drosophila*.

A) Comparison of baseline spike rate of IPCs between virgin females, mated females, and males. **B)** Comparison of baseline spike rate between *Drosophila* of different age groups. d = days, n = number of individual IPC recordings. Each circle represents an individual IPC, error bars indicate median (circle) and interquartile range (IQR, bars). p-values from Wilcoxon rank sum test. **C)** Percentage survival of flies on different diets. After 24 h of starvation, flies were kept on a high glucose (HG), high protein (HP) or standard diet (SD). Data points represent sum of two replicates of 20 flies per condition, in total we used N = 40 flies per condition.

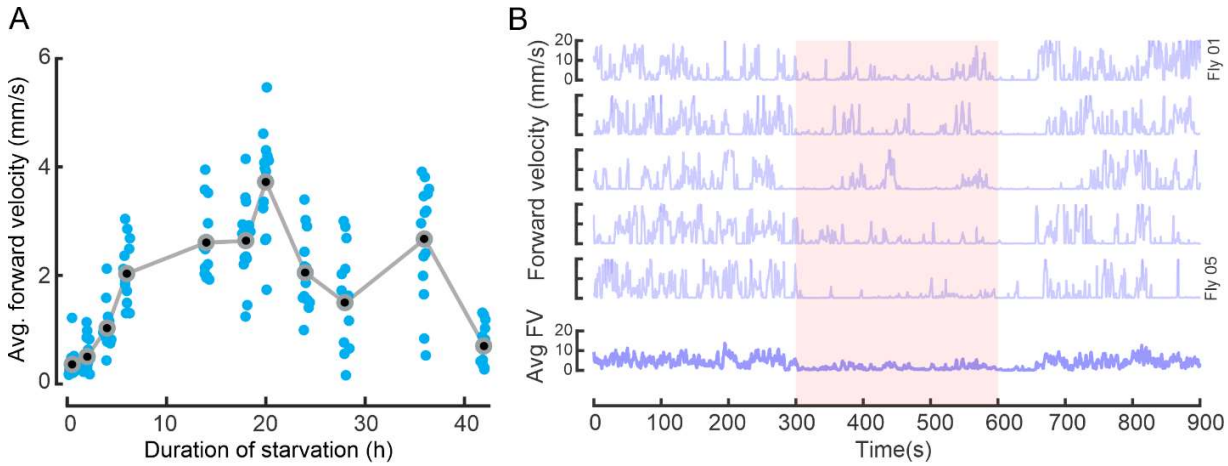

Figure S2: Starvation duration and OAN activation affect foraging behavior.

A) Average forward velocity of flies during different periods of starvation. N = 20 flies per condition, each circle represents an individual fly, gray circles and lines represent means. **B)** Upper panel: Forward velocities of five example flies displaying stopping behavior during OAN activation. Examples are shown for the fifth activation cycle. Lower panel: Average forward velocity of all flies from one replicate (N = 20). Red bar represents OAN activation.

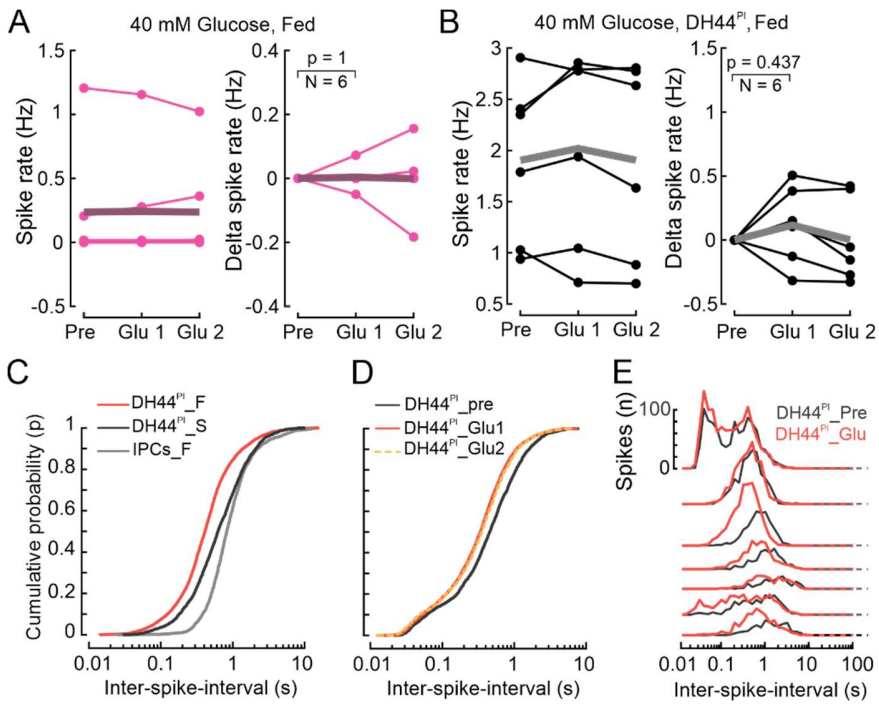

Figure S3: Glucose perfusion does not affect the activity of IPCs and DH44^{PI}Ns in fed flies but shifts spike activity patterns in DH44^{PI}Ns.

Spike rate and delta spike rate of IPCs and DH44^{PI}Ns in different conditions. **A)** IPCs in fed flies under 40 mM glucose perfusion. **B)** DH44^{PI}Ns in fed flies under 40 mM glucose perfusion. Pre, five-minute recording in glucose-free extracellular saline, Glu1 and Glu2, two subsequent five-minute recordings in glucose-rich extracellular saline, starting eight minutes after onset of glucose perfusion. Each circle represents an individual fly, thick line represents the grand mean of all flies, p-values were calculated via Wilcoxon signed-rank test. Spike rates were averaged for each fly within a five-minute window, delta spike rates were calculated by subtracting the mean spike rate during the Pre window from all subsequent means. **C)** DH44^{PI}N spike activity patterns change in fed and starved flies. Cumulative probability distribution of the ISI in DH44^{PI}Ns and IPCs. F = fed flies, S = starved flies. Distributions were compared using the two-sample Kolgomorov-Smirnov test (DH44^{PI}_F vs IPCs_F: $p = 1.5e^{-216}$; DH44^{PI}_F vs DH44^{PI}_S: $p = 2.5e^{-86}$; DH44^{PI}_S vs IPCs_F: $p = 7.4e^{-51}$). **D)** Cumulative probability distribution of the ISI in Pre, Glu 1 and Glu 2 windows reveals that DH44^{PI}N activity became more bursty during glucose perfusion. Distributions were compared using the two-sample Kolgomorov-Smirnov test (DH44^{PI}_pre vs DH44^{PI}_Glu1: $p = 6.5e^{-30}$; DH44^{PI}_pre vs DH44^{PI}_Glu2: $p = 2.3e^{-21}$; DH44^{PI}_Glu1 vs DH44^{PI}_Glu2: $p = 0.05$). **E)** DH44^{PI}N spike activity patterns change during glucose perfusion. Inter-spike-interval (ISI) for DH44^{PI}Ns before (Pre) and during (Glu) 40 mM glucose perfusion.

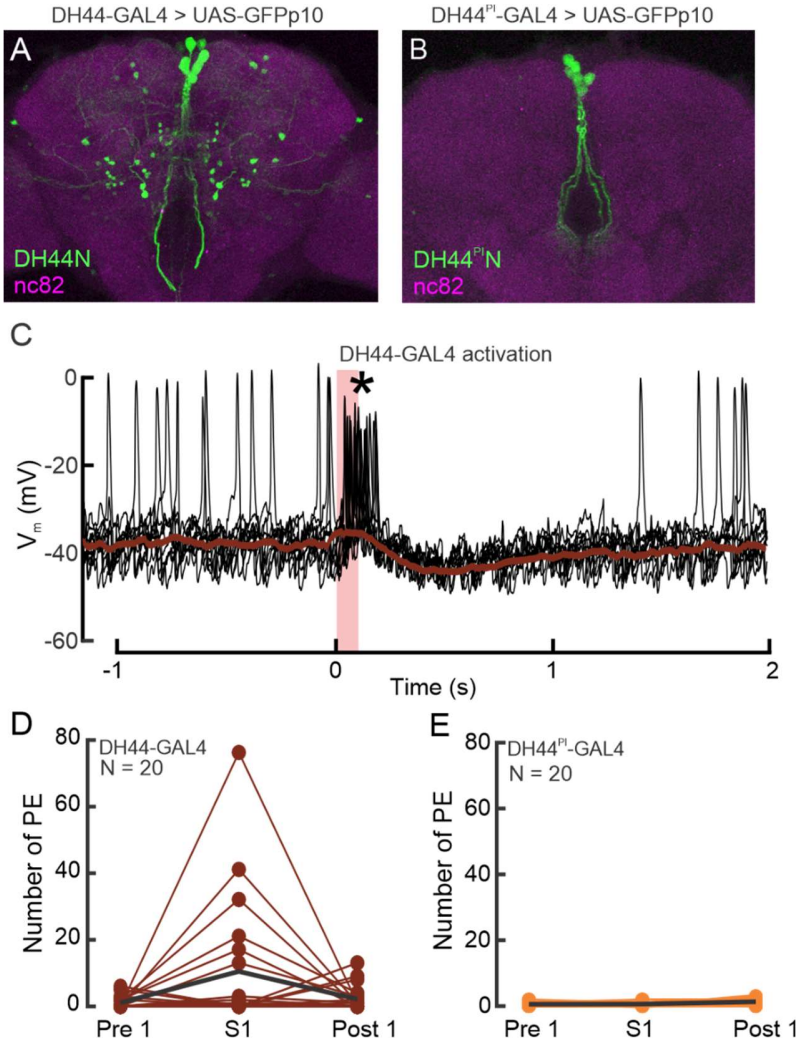

Figure S4: Effects of differential activation of DH44Ns and DH44^{PI}Ns on IPCs and behavior.

A) and **B)** Labeling of DH44Ns in the brain using a broad (DH44N, A) and a sparse (DH44^{PI}N, B) *GAL4* driver line and a *UAS-GFPp10* reporter, respectively. GFP was enhanced with anti-GFP (green), brain neuropils were stained with anti-nc82 (magenta). **C)** Example recording of an IPC during optogenetic activation of the broad DH44N driver line. In this one example, we observed strong activation of the IPC (marked by asterisk) during DH44N activation. However, about ~100 ms after activation, the IPC was inhibited similar to all other recordings (see also Fig 4B). **D)** and **E)** Number of proboscis extensions (PE) before (Pre 1), during (S1), and after the first LED pulse (Post 1), while activating DH44Ns (D) or DH44^{PI}Ns (E) , respectively, in freely walking flies in the UFO. PEs were counted manually. Thick, black lines represents the grand mean.

Table S1: p-values values for statistical comparisons in Figure 2.

p-values were determined using the Wilcoxon rank-sum test. 1-5 represent the five activation cycles in Figure 2E, H and K. 'Activation' shows the p-values comparing average forward velocity pooled across activation trials (Figure 2L).

Genotype	1	2	3	4	5	Activation
TDC2>CsChr	**$2.1e^{-05}$**	**$1.3e^{-10}$**	**$7.7e^{-12}$**	**$8.3e^{-12}$**	**$3.6e^{-12}$**	**$6.8e-^{48}$**
DILP2>CsChr, Fed	**0.0256**	0.8694	0.5705	0.1867	0.1507	**0.0133**
DILP2>CsChr, Starved	**$3.4e^{-09}$**	**$7.2e^{-06}$**	**$1.2e^{-06}$**	**0.0021**	**0.0042**	**$1.0e^{-20}$**

Table S2: p-values values for statistical comparisons in Figure 2.

p-values were determined using Wilcoxon rank-sum test. P1-P5 represent the 'post activation' windows in Figure 2E, H and K. 'Post activation' contains the p-values comparing average forward velocity pooled across all trials (Figure 2M).

Genotype	P1	P2	P3	P4	P5	Post
TDC2>CsChr, Fed	**$6.5e^{-13}$**	**$1.7e^{-13}$**	**$8.9e^{-13}$**	**$4.7e^{-13}$**	**$7.2e^{-12}$**	**$7.3e^{-58}$**
DILP2>CsChr, Fed	0.4357	0.9958	0.2543	0.7868	0.3874	0.6170
DILP2>CsChr, Starved	**$5.3e^{-06}$**	**0.0003**	**0.0008**	0.2322	0.4540	**$1.7e^{-8}$**

Table S3: p-values values for statistical comparisons in Figure 4

p-values were determined using Wilcoxon rank-sum test. 1-5 represent the five activation cycles in Figure 4K and N.

Genotype	1	2	3	4	5
DH44>CsChr	**$1.9e^{-11}$**	**$2.1e^{-12}$**	**$8.6e^{-08}$**	**$4.5e^{-06}$**	**$2.8e^{-06}$**
$DH44^{Pl}$>CsChr	**0.0001**	**0.0022**	0.0540	**0.0156**	**0.0015**

Table S4: p-values values for statistical comparisons in Figure 4.

p-values were determined using Wilcoxon rank-sum test. P1-P5 represent the 'post activation' windows in Figure 4K and N.

Genotype	P1	P2	P3	P4	P5
DH44>CsChr	**$2.3e^{-10}$**	**$2.7e^{-13}$**	**$2.8e^{-10}$**	**$4.0e^{-08}$**	**$6.7e^{-10}$**
$DH44^{Pl}$>CsChr	0.2711	0.1895	0.9044	0.0602	**0.0054**

Supplementary video S1: Behavioral effects of optogenetic OAN activation on *Drosophila* locomotor activity in the UFO.

Example video of OAN-activated flies walking in the UFO during the fifth activation cycle. The white box indicates when the optogenetic stimulation light is on. The video includes one-minute before activation (P4 in Fig 2E), 5-minutes of activation (5 in Fig 2E), and one-minute after activation (P5 in Fig 2E). During OAN activation, the forward velocity decreased significantly, including several pausing episodes.

Supplementary video S2: Behavioral effects of the optogenetic activation protocol on the locomotor activity of Empty-Gal4 control flies in the UFO.

Example video of control flies responding to the light pulse used for optogenetic activation during the fifth activation cycle. These flies were recorded in parallel to the OAN-activated flies in Video S1. Details are the same as for Supplementary video S1.